Received: 16 December 2021 | Revised: 13 April 2023 | Accepted: 16 April 2023

DOI: 10.1002/esp.5606

RESEARCH ARTICLE

ESPL WILEY

Genesis of subglacial triangular-shaped landforms (murtoos) formed by the Fennoscandian Ice Sheet

Joni Mäkinen[1] | Kari Kajuutti[1] | Antti E. K. Ojala[1] | Elina Ahokangas[1] | Aleksi Tuunainen[2] | Markus Valkama[2] | Jukka-Pekka Palmu[2]

[1]Department of Geography and Geology, University of Turku, Turku, Finland

[2]Geological Survey of Finland, Espoo, Finland

Correspondence
Dr. Joni Mäkinen, Department of Geography and Geology, University of Turku, FI-20014 Turku, Finland.
Email: jonmak@utu.fi

Funding information
Academy of Finland, Grant/Award Numbers: 322243, 322252

Abstract

The purpose of this paper is to describe the internal structure and composition of recently discovered subglacial landforms called "murtoos" in order to interpret their formative processes and depositional environment. So far, murtoos have only been reported from Finland and Sweden, but they probably exist in all areas covered by past ice sheets. Murtoos mainly occur in fields along subglacial meltwater routes or corridors in close relation to eskers and ribbed moraine tracts. Murtoos were excavated perpendicular to the long axes of the triangular murtoo heads in six locations. Murtoos were found to be composed of silt/clay-poor, sandy and gravelly diamictons interbedded with sorted sediments, and are suggested to be produced by pulsed, highly sediment-concentrated flows during weak glaciotectonic deformation, indicating effective pressure close to zero. Murtoos can be divided into three main depositional units: 1) the core, 2) the murtoo body and 3) the murtoo mantle. The initial deposition of murtoos took place in a network of low canals and conduits or cavities with fluctuating stream flow likely over 50 km from the ice margin. Murtoos reveal an increasing influence of subglacial meltwater flow in rapidly widening broad and low conduits with increasing sediment transport over short distances. The results of this work suggest that murtoos were formed time-transgressively over yearly meltwater cycles in a semi-distributed drainage system not recognised before, in which was high-pressure porewater conditions with rapid mobilisation of subglacial saturated sediments, a critical factor in the development of semi-efficient drainage. Murtoos are suggested as missing element between distributed and channelised drainage systems not included in current glaciohydrological models or even in the theoretical basis of glacial hydrology.

KEYWORDS
geomorphology (glacial), glaciology, murtoo, Quaternary, sedimentology, subglacial hydrology

1 | INTRODUCTION

Using light detection and ranging (LiDAR) data for construction of digital elevation models (DEMs), Finnish and Swedish researchers (e.g., Mäkinen et al., 2017; Peterson et al., 2017) have discovered triangular-shaped subglacial landforms that have been named "murtoos" (Ojala et al., 2019). The morphometrics of murtoos, as well as their distribution within the boundaries of the former Fennoscandian Ice Sheet (FIS) in Finland and Sweden, have been published by for example, Ojala et al. (2019, 2021). However, the structure and formational processes of murtoos have remained poorly understood because of limited sedimentological data. Such has, however, recently only been reported from southern Sweden (Peterson-Becher & Johnson, 2021), here formed at deglaciation during the warming climate of the Bølling–Allerød interstadial prior to the Younger Dryas. Murtoos have additionally been associated with

the rapid melting and retreat of the FIS north of the Younger Dryas ice marginal zone in Finland (Ojala et al., 2019).

Murtoos are mostly less than 5 m in height, characterised by sandy diamictons interbedded with sorted sediments. The triangular heads of triangular-type murtoos, and also the heads of chevron-type and lobate-type murtoos (Ojala et al., 2019), point down-flow and are thus indicative of the local ice-flow direction. Previously, murtoos have either been mapped as hummocky moraines without mentioning their triangular heads, or just left unmapped as part of the ground moraine cover. A characteristic landscape feature of murtoo fields is the abundance of large boulders on their surfaces.

This paper focuses on the internal architecture and sediment composition of murtoos formed during the rapid Holocene melting and deglaciation of the FIS in Finland, this in order to interpret their formative processes and environment. These results are compared with the sedimentary characteristics from the south-Swedish murtoos investigated by Peterson-Becher & Johnson (2021).

2 | STUDY AREA

2.1 | Murtoo distribution

The distribution of well-defined triangular-shaped murtoos in Finland had been mapped by Ojala et al. (2019) and Ahokangas et al. (2021) (Figure 1). Murtoos mainly occur in three larger clusters, two of these located along the track of the Finnish Lake District Ice-Lobe (FLDIL) (Figure 1), while a third cluster in SW Finland is associated with the eastern margin of the Baltic Sea Ice Lobe (BSIL). Murtoos typically occur as fields along subglacial meltwater routes or corridors

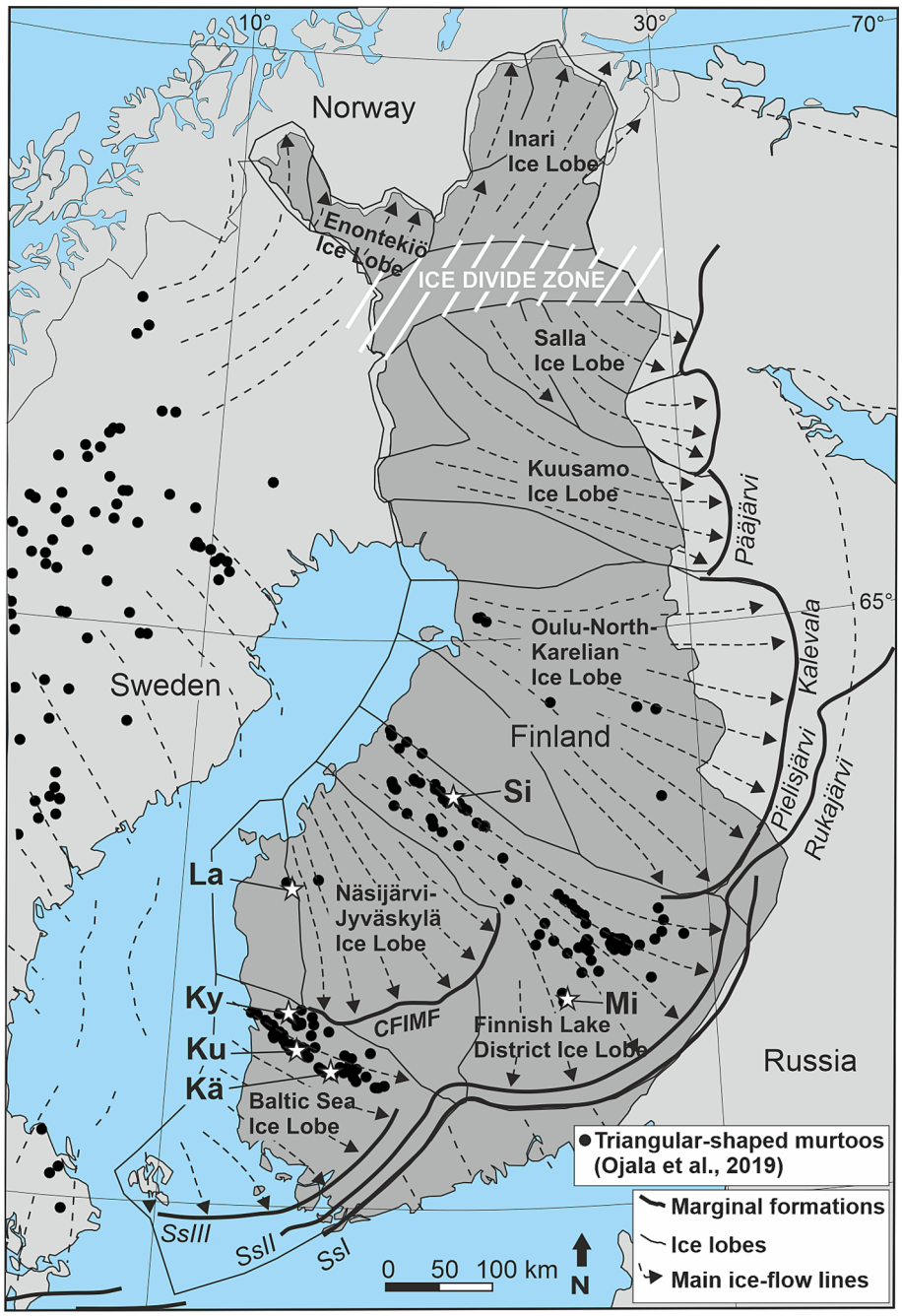

FIGURE 1 Distribution of murtoos (Ojala et al., 2019), ice-stream lobes and excavated study sites (stars) in Finland. Abbreviations: Kä, Kämmäkkä; Ku, Kullaa; Ky, Kynäsjärvi; La, Laihia; Mi, Mikkeli; Si, Sievi.

(Figure 2) in close association with eskers and ribbed tracts (Ahokangas et al., 2021). The study sites presented here (Figure 1, Table 1) include the main clusters of murtoo fields in southern Finland, which represent areas with diverse glaciodynamic settings. The Mikkeli site is located in an area that experienced a supra-aquatic deglaciation (Ojala et al., 2013), whereas the other sites are located in

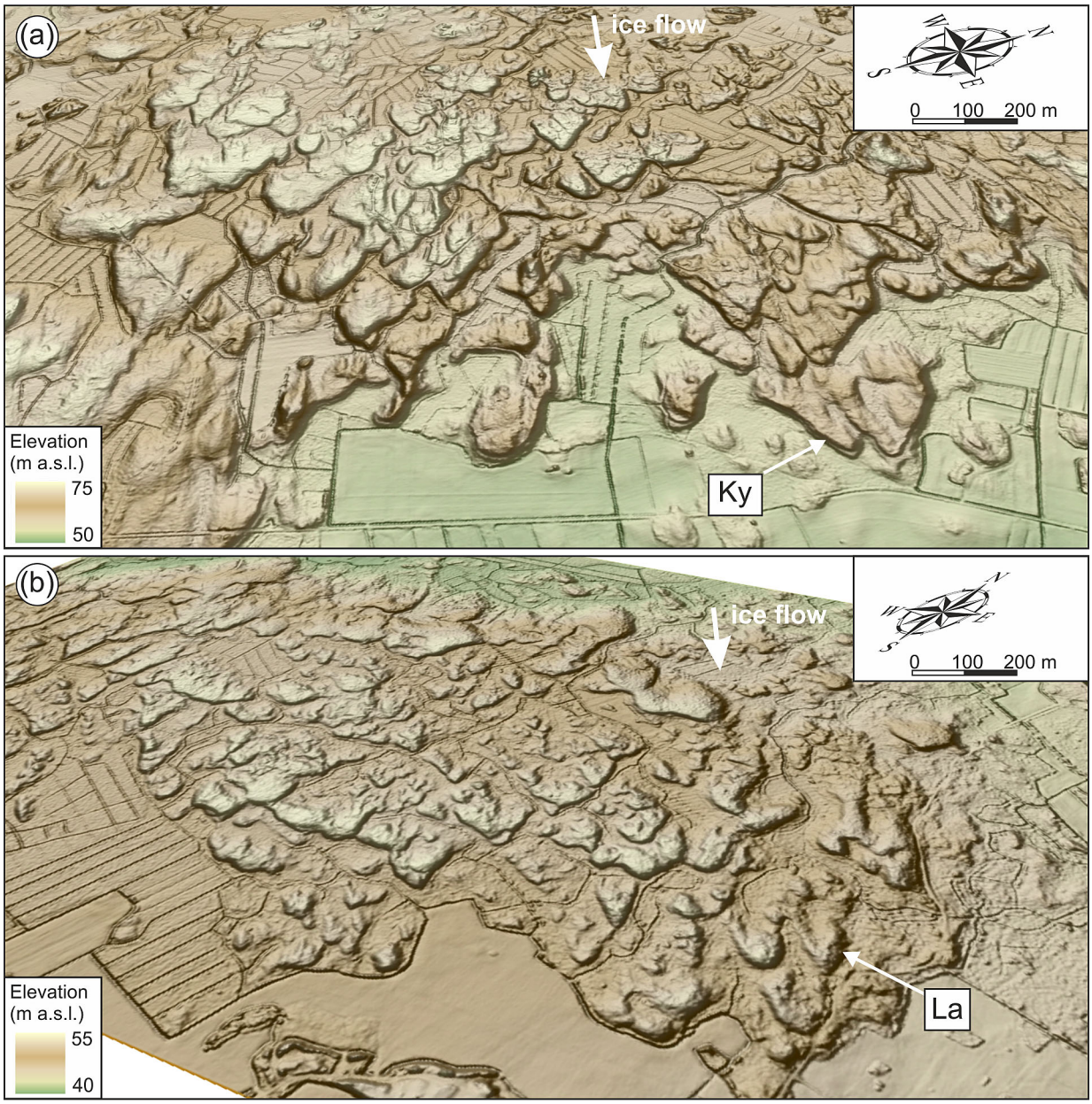

FIGURE 2 Examples of murtoo fields shown by oblique hill-shaded views of LiDAR DEMs. (a) the Kynäsjärvi (Ky) site, and (b) the Laihia (La) site. Excavated murtoos are indicated by arrows. Note the overlap and up-ice gradation of murtoos and the distribution of more triangular-shaped murtoos in the middle of the field in Kynäsjärvi, indicating a higher concentration of meltwater flows. (Background map source: LiDAR DEM, © National Land Survey of Finland, 12/2021).

TABLE 1 Dimensions and location of the excavated murtoos.

Murtoo	Length (m)	Width (m)	Height (m)	Base	Coordinates (WGS-84, N / E)
Kämmäkkä	28	27	1.5–2.0	bedrock	61,226,597,342° / 22,918,321,369°
Kullaa Ku1	104	52	2–3	bedrock	61,422,148,353° / 22,279,471,135°
Kullaa Ku2	86	75	1.5–2.0	till	61,421,975,027° / 22,281,731,334°
Kynäsjärvi	91	83	4	?	61,715,115,258° / 22,189,284,267°
Laihia	110	70	2.0–2.5	till	62,848,103,726° / 22,111,927,236°
Mikkeli	112	83	3.0–3.5	bedrock	61,830,504,706° / 27,252,043,707°
Sievi	127	130	4	till?	63,679,970,881° / 24,903,419,399°

areas where the ice-stream margin ended in a proglacial water body of the Baltic Sea basin at deglaciation. All excavation sites are located within the Svecofennian basement rocks domain, mainly composed of biotite paragneiss and tonalite (Lehtinen et al., 2005).

2.2 | Geomorphological setting of study sites

LiDAR-based DEM images showing the topographical setting of the excavated murtoos, and selected geomorphic features are presented in the supplementary material (Figure S1a–f), with examples from the Kynäsjärvi (Ky) and Laihia (La) sites given in Figure 2. The Kullaa (Ku) and Kynäsjärvi (Ky) sites are within 2.0- to 2.5-km-wide subglacial meltwater routes that delineate the margins of the Satakunta hummocky/ribbed moraine area within the Loimaa sublobe of the BSIL (Mäkinen et al., 2017). The Kämmäkkä (Kä) site, also located within the Loimaa sublobe, forms part of an approximately 1.0-km-wide, weakly developed meltwater route up-ice from a small tributary esker. The Laihia murtoo is located next to an esker within a murtoo field about 2.0 km^2 in size that is not part of a subglacial meltwater route but lies proximal to an area that has been interpreted as a cold-based area within the Suupohja district (Pitkäranta, 2009). The Mikkeli (Mi) site is situated along a subglacial meltwater route next to an esker and has small sporadic murtoo clusters between streamlined terrains of the FLDIL. The excavated murtoo in Sievi (Si) is situated within a 0.5- to 1.0-km-wide subglacial meltwater route that cuts through a field of ribbed moraine and subglacial hummocky moraine within the margin of a drumlinised ice-flow corridor along the trunk of the FLDIL (Ahokangas & Mäkinen, 2014; Vérité et al., 2021). The distances from the excavated murtoos to the nearest esker vary between 0.8 and 3.5 km for those sites (Kullaa, Laihia, Mikkeli, Sievi) where the murtoo route occurs alongside an esker, but between 8.2 and 27.2 km for the sites (Kämmäkkä and Kynäsjärvi) that join an esker down-ice.

3 | METHODS

Murtoo landforms at six different sites (Figure 1) were systematically excavated perpendicular to the long axes of the triangular murtoo heads, that is, also close to perpendicular to the former ice flow direction. The main trenches about 20–45 m long and 2–3 m wide were dug about 20–30 m upflow from murtoo tips. With exception for the Kynäsjärvi site (Figure 2), all other trenches cut through the steeply dipping murtoo margins. Depending on landform relief, the highest vertical sections of the trench walls were 3–5 m, this depth partly also determined by safety precautions. The intension at excavation was to retain relatively steep section walls but avoid excess leakage of groundwater into the trenches. The number of surface boulders (>0.5 m in diameter) per 100 m^2 was calculated from the central part of murtoo close to the trench.

In addition to the main trenches, smaller test pits were excavated into the proximal side of murtoos in Sievi and Mikkeli, and into the front of the tip in Mikkeli. The trenches were first located with a hand-held GPS and levelled by using a levelling instrument in order to draw cross-sections in the field. The trenches were marked with a ground-fixed measuring tape to locate the observations and measurements along the cross-section. The sedimentological work aimed at discerning and mapping architectural/depositional units, supplemented with photo mosaics, and to carry out detailed lithofacies descriptions with simplified lithofacies classification (Table 2). Stone percentage counts (clasts >64 mm) were performed using a 1 × 1 m and 10 × 10 cm gridded net. Palaeoflow directions were measured from ripple cross-laminations and trough-shaped structures (continuation determined from both trench walls), supplemented with dip measurements of non-disturbed sand beds. Clast fabric orientation (azimuth and dip) was usually performed on sets of 50 clasts, 2–10 cm long with a minimum elongation ratio of 2:1. At a few occasions, this was reduced to minimum of 25 clasts. Macrofabric data were processed using Orient 3.13.0 software. Representative macrofabrics were attained from 7 to 12 locations along the trenches at the Kynäsjärvi, Laihia and Mikkeli sites.

TABLE 2 Lithofacies codes used in this study.

D,G,S,F	Mean grain size (Diamicton, gravel, sand, fines (clay to silt)
(bo,g,s,f)	Subordinate grain size (bouldery, gravelly, sandy, with fines)
m	massive
mm	massive, matrix-supported
mc	massive, clast-supported
mng	massive, normal grading
s	stratified
cs	crudely stratified
r	ripple cross-lamination
l	lamination
i	inclined bedding
d	deformed
(t)	trough-shaped set

Grain-size distributions were made on 53 samples (max. clast size 64 mm) by means of wet-sieving or dry-sieving. The clay fraction of selected samples (n = 39) was determined by sedigraph analyses (Micromeritics SediGraph III Plus with the MasterTech 52 autosampler, Norcross/GA, USA) from the sieved material finer than 0.063 mm. Grain-size distribution curves (grain sizes in the Udden–Wentworth scale), and also reference data (Table S3) from the regional tills by the Geological Survey of Finland, are presented as supplementary material (Figure S2a-e). The roundness of pebble-sized (8–64 mm) clasts of the sieved samples was visually determined against the 6-class roundness scale of Powers (1953) from samples taken at five sites (Kullaa, Kynäsjärvi, Laihia, Mikkeli and Sievi), in total 2,185 clasts (Table 3). Otherwise, the roundness of cobbles and boulders was visually compared with the roundness scale of Powers (1953) in the field.

4 | RESULTS

4.1 | Kullaa (Ku)

At Kullaa, a 36-m long section (Ku2) was excavated through a low-relief murtoo head, approximately 1.5–2.0 m high (Figure 3). An

TABLE 3 Roundness (Powers, 1953) of sieved murtoo-sediment clasts, 8–64 mm in size.

Site	Angular (%)	Subangular (%)	Subrounded (%)	Rounded (%)	Clasts (total 2,185)
Kullaa	29.5	62.4	7.9	0.2	604
Kynäsjärvi	29.2	63.1	7.7	0.0	377
Laihia	13.7	75.9	10.2	0.2	431
Mikkeli	20.2	75.4	4.4	0.0	248
Sievi	15.4	76.8	7.8	0.0	525
Average	21.6	70.7	7.6	0.1	

additional pit 18 m long and 2.0–3.0 m deep was dug down to an ice-abraded bedrock knob in the NE margin of another murtoo head (Ku1) located up-ice from the section Ku2 (Figures 3a,c). The SW sides of both murtoos are bordered by a large fan-shaped hollow. Excavated murtoo sediments are divided into three architectural/depositional units.

4.1.1 | Depositional unit 1

Section Ku2 reaches the compact, silty and bouldery diamicton (till) beneath the murtoo sediment proper (Figure 3b). Unit 1 forms a broad, gently arched architecture with the largest boulders clustered in the central bottommost part of the section (Figure 3b). It is mainly composed of sandy, massive/matrix-supported to crudely stratified and poorly sorted pebble gravel with occasional small boulders. The pebble-sized clasts are dominantly angular to subangular, whereas larger clasts are subangular to subrounded. Stratification is mainly due to crude gravel clast layers.

Unit 1 in the section Ku1 reveals inclined, crudely stratified gravel beds, including open-work gravel and small boulders (Figure 3d). These sediments have a basal contact to ice-abraded bedrock.

4.1.2 | Depositional unit 2

The lower part of Unit 2 (subunit 2a) has similar gravels to those in Unit 1, but is sandier, including partly preserved interbeds (5–20 cm thick) of silty fine- to medium-grained sand with deformed lamination (Figure 4a). The latter beds have gradational upper contacts and are often somewhat dislocated and broken into streaks and rafts (Figure 4b). However, the sand horizons are traceable across the section (Figure 3b). The subunit also includes patches of well-sorted granule to fine-pebble gravel, 2–3 cm thick. The largest clasts are commonly <0.2 m in diameter. The massive to crudely stratified gravels contain 3.0–5.0% mud and only 0.1–0.2% clay.

Trough-shaped diamictons cut the NE margin of Unit 1 and the interbedded part of subunit 2a, reaching the till beneath the murtoo sediments (Figures 3b and 5). These diamictons have amalgamated contacts and are massive/matrix-supported to locally clast-supported with small boulders or sandy and pebbly, crudely stratified with pebble–cobble lags (Figure 5). A partly preserved layer of massive mud (Fm) tops the stacked diamictons (Figure 5). Furthermore, Subunit 2a in the NE slope of the murtoo includes a marginal trough composed of NE-dipping (030–070°/10–20°), crudely stratified cobbly gravels and clast-supported pebble gravels (Figures 3b and 4c). These inclined gravels are topped by an upslope-climbing coset of current ripples 3–5 cm high (set boundaries dip 100°/10°) in medium to coarse sand (Figure 4d).

In pit Ku1, subunit 2a shows up as sandy, poorly sorted and crudely stratified gravel beds with occasional boulders or as sandy, massive/matrix-supported diamicton beds having a crude trough shape. It is topped by a deformed, silty fine-grained sand layer with clay laminations (S(f)ld, Figure 3c).

The upper part of Unit 2 in section Ku2 (subunit 2b) is composed of trough-shaped sets of poorly sorted, massive/matrix-supported or massive/clast-supported, weakly normal-graded pebble-gravel beds (Figures 3b and 4e), as well as stratified sands. The sets are 1–4 m wide and up to 0.5 m thick and carry occasional small boulders. Set contacts are mostly amalgamated and have weakly developed cobble lags (Figure 4a, e). Some gravel beds carry small rafts/intraclasts of sand. The SW margin of subunit 2b is cut by trough-shaped diamictons with boulder lags, whereas the NE margin displays a relatively thin diamicton, containing cobbly gravel pockets (load structures) intruding into the fine-grained and rippled beds on top of subunit 2a (Figure 4f).

In pit Ku1, subunit 2b consists of crudely trough-shaped beds of sandy-gravelly massive/matrix-supported diamictons with occasional boulders. These beds transform down-ice into just one 5.0-m wide and approximately 1.0-m thick diamicton with a trough-shaped basal outline. At its margin is an almost vertically dislocated sand patch, removed from the underlying silty fine-grained bed (Figure 3d). The patch has a sharp/erosional contact towards the trough, but a mixed/injected structure towards the centre of the murtoo, indicating deformation during the deposition of the diamicton.

4.1.3 | Depositional unit 3

The murtoos and their marginal channels, as well as the adjacent murtoo-related ridges (Ku3, Figure 3a) are draped by a loose, poorly sorted massive/matrix-supported to crudely stratified sandy diamicton with boulders (Figures 4a and 5). The lower part of the unit within the marginal channel reveals crudely stratified pebble gravel (Figure 5), and the lower contact to Unit 2 is amalgamated or, in places, sharp/erosional. However, much of the original sedimentological characteristics of the rather thin Unit 3 has been changed because of the physical/chemical soil forming processes, leading to podsol formation within the present forest bed. The murtoo surfaces exhibit approximately 10–15 boulder per 100 m^2.

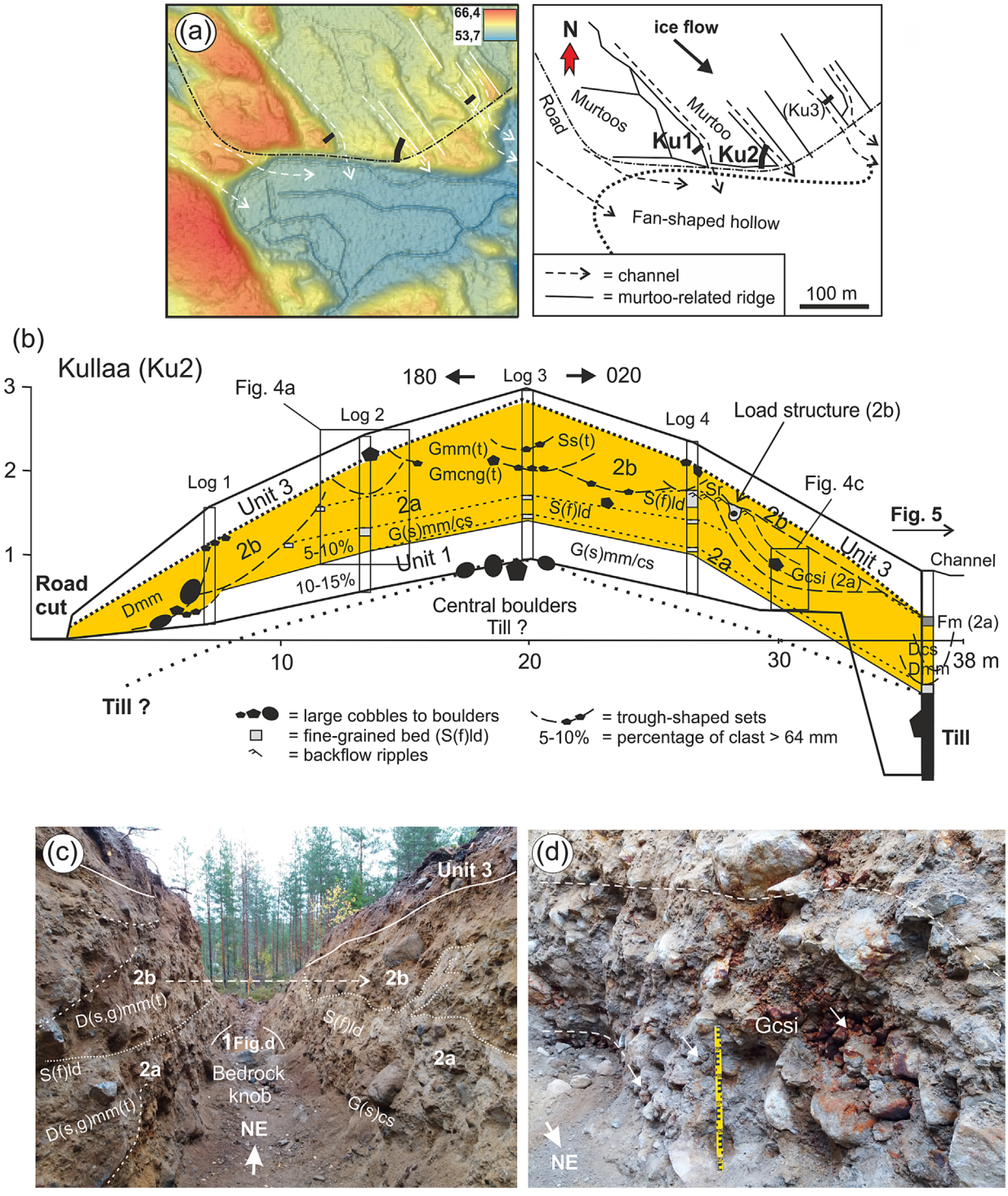

FIGURE 3 The Kullaa murtoos. (a) Location of trenches Ku1 and Ku2. Note the relationship between murtoos, murtoo-related ridges (Ku 3, Ojala et al., 2021), meltwater channels and a large fan-shaped hollow. Colour ramp in m a.s.l. (background map source: LiDAR DEM, © National Land Survey of Finland, 12/2021). (b) a simplified sketch of the section Ku2 (not all large cobbles/boulders are marked) with Unit 2 in yellow, forming the murtoo body. (c) the NE margin of a murtoo (Ku1) excavated down to an ice-abraded bedrock knob. Note the location of Unit 1 (core) on the side of the bedrock knob and the transition of diamictons/D(s,g)mm(t) in subunit 2b into large trough-shaped diamicton with marginal deformed sands. Dashed lines indicate set boundaries and dotted line the top of subunit 2a (S(f)ld). (d) Inclined, crudely stratified open-work gravel beds (Gcsi) in Unit 1 (delineated by dashed lines) lateral to the bedrock knob. These are the coarsest core deposits of all the studied sites.

4.2 | Kynäsjärvi (Ky)

The Kynäsjärvi murtoo was excavated close to its eastern head with a 40-m long section, the northern part of it cutting the northern margin of the murtoo, whereas the southern part of the section follows its southern margin (Figure 6a). In addition was a 7-m long trench excavated towards the ice-flow direction (Figure 6a). The murtoo sediments are 5 m thick with an arched core at least 2.0–2.5 m thick and 20 m wide. The murtoo has two low shore terraces incised into its margins (Figure 6c), which indicate the lowering of the level of Lake Kynäsjärvi by 4 m during the 19th century. Excavated murtoo sediments are divided into three architectural/depositional units.

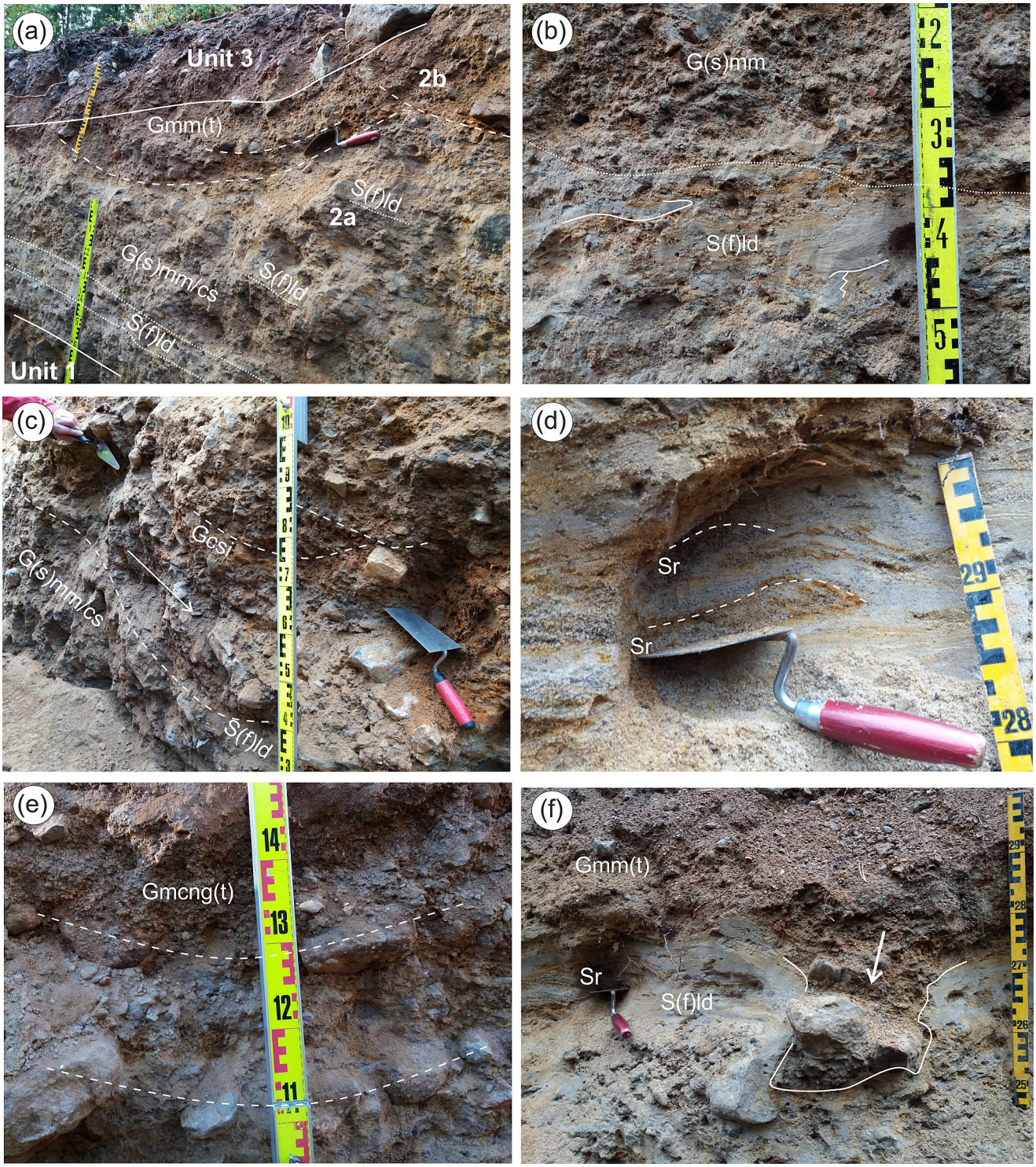

FIGURE 4 Key sedimentary structures from the section Ku2 of the Kullaa murtoo. (a) Depositional units within the SW side of the murtoo. Dashed lines indicate set boundaries and dotted lines the boundaries of facies S(f)ld. (b) Deformed (solid lines) fine-grained interbeds (S(f)ld) with streaks in gravel within subunit 2a. (c) Crudely stratified gravel with inclined clast-supported beds (Gcsi, dashed lines indicate bed boundaries) within the NE margin of the murtoo. (d) Climbing backflow ripples (Gcsi) on top of inclined, crudely stratified gravels within the NE margin of the murtoo (see Figure 4c). (e) Trough-shaped diamictons of subunit 2b with cobble lags and massive/clast-supported gravel including normal grading Gmcng(t). (f) Rippled fine-grained beds deformed by a downward-pushed diamicton pocket with cobbles (load structure, solid line) (see Figure 3b).

4.2.1 | Depositional unit 1

Unit 1, though poorly exposed, is composed of massive to crudely stratified gravel beds in crudely trough-shaped sets with basal cobble lags. The gravel beds carry rafts or dislocated patches of fine to medium sand, usually with contorted lamination. In places, the sand beds are better preserved and 5–25 cm thick, including current ripples (Figure 7a). The largest clasts are about 0.3 m in diameter and are dominantly subangular to subrounded.

FIGURE 5 Picture of a pit located between the murtoo and murtoo-related ridge at the NNE end of section Ku2 (see Figure 3b). The pit reveals a silty bouldery diamicton (till) at the bottom, overlain by partly preserved unit 1 and subunit 2a composed of trough-shaped diamictons of varying structure topped by poorly preserved bed of massive mud (Fm). The massive/matrix-supported diamicton of unit 3 with discontinuous bed of crudely stratified gravel in the lower part of the unit is altered by forest bed processes. Solid lines display unit boundaries, dashed lines set boundaries and bo indicates the position of a removed boulder. Photo towards NNE.

4.2.2 | Depositional unit 2

With an amalgamated contact to Unit 1, subunit 2a is composed of a crudely stratified gravelly and bouldery diamicton, associated with discontinuous, deformed patches of laminated sand beds inclined towards the murtoo margin (Figure 6c). Clast fabrics from the central lower part of the subunit reveal bimodal distributions that are both parallel and transverse to flow direction (Figure 6d). The number of boulders increases downslope (the largest ones 0.6–1.0 m in diameter), which probably indicates a larger depositional space along the murtoo margins (Figures 6c,e). In places, the intraclasts have been chaotically mixed with coarser sediments (Figure 7b). Sand patches are usually deformed, including contorted laminations, large out-sized clasts that cut through the sand (Figure 7c), and clasts pushing against sand intraclasts associated with small-scale faulting (Figure 7d).

The southern part of Unit 2 can be divided into two subunits (2a and 2b) by a laterally more continuous, but poorly preserved, muddier laminated/deformed sand bed that has been mixed into the overlying subunit 2b (Figure 7e). The northern margin of subunit 2a is topped by a massive and clay-rich bed of mud, approximately 10–20 cm thick (Figure 6c).

The upper part of Unit 2 (subunit 2b) is composed of massive/matrix-supported to crudely stratified sandy diamicton beds with 0.7–1.0% clay and a low clast content (5%) (Figures 6c,e and 7b). In the uppermost part, the diamicton forms trough-shaped sets a few meters wide that are diagonally oriented towards the murtoo margin with weakly aligned clast fabrics (Figure 6c,d). However, the trough-shaped diamicton along the northern murtoo margin has clast fabric mainly parallel to the trough axis, indicating flow towards the murtoo tip (Figure 6b,e). Subunit 2b also contains a large boulder that has been pushed down, deforming the underlying subunit 2a (Figure 7f).

The pebble-sized clasts in Units 1 and 2 are dominantly angular to subangular (similar to Kullaa clasts, Table 3), whereas larger clasts in the section are subangular to subrounded. According to measurement

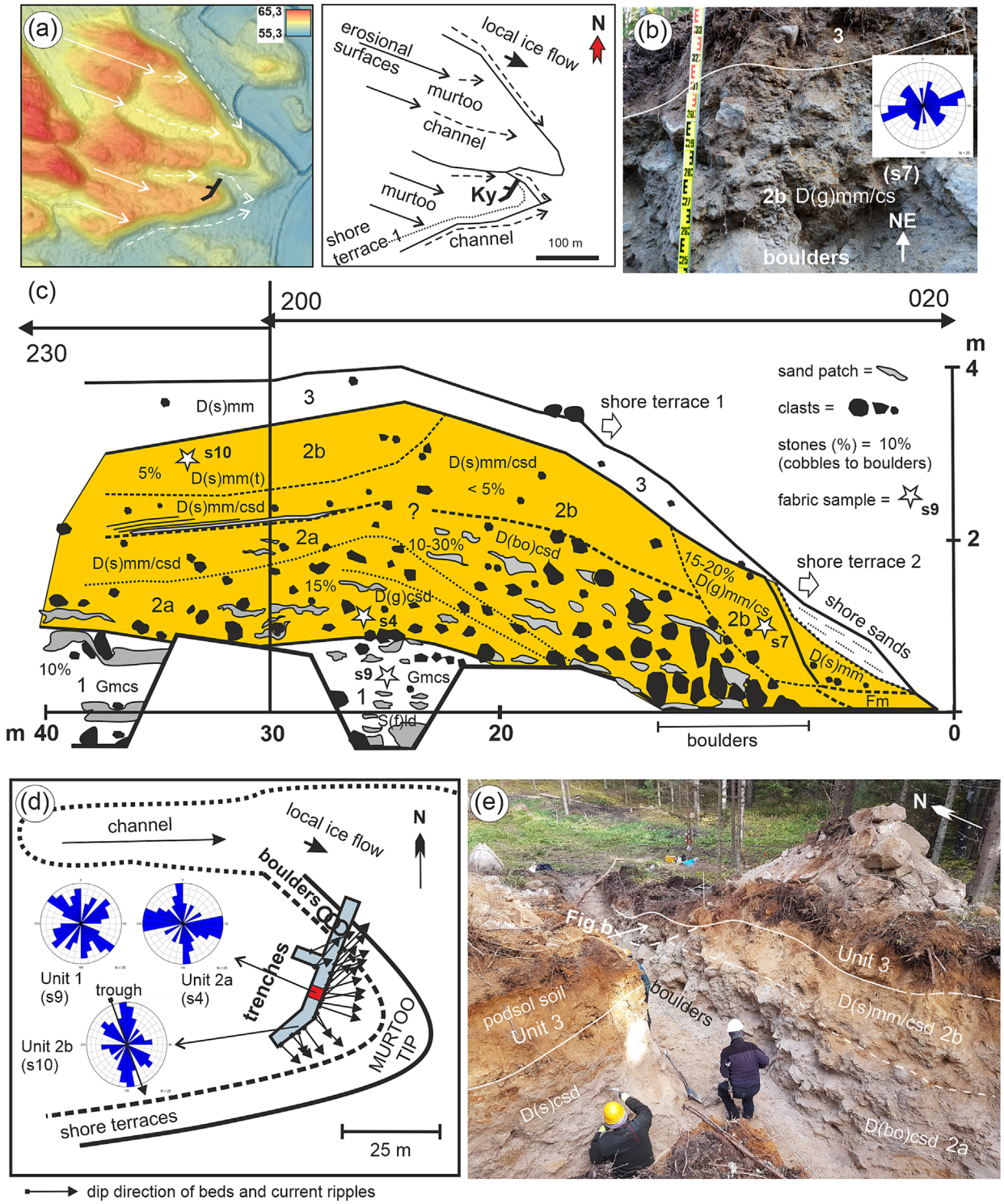

FIGURE 6 The Kynäsjärvi murtoo. (a) Location of the trench (Ky) in relation to erosional surfaces of the overlapping murtoos (solid arrows), meltwater channels (dashed arrows) and shore terraces. Colour ramp in m a.s.l. (background map source: LiDAR DEM, © National Land Survey of Finland, 12/2021). (b) Trough-shaped diamicton (D(g)mm/cs) along the NNE margin of the murtoo. Marginal channelised flow with the parallel preferred orientation of elongated clasts (fabric n = 25) towards the tip of the murtoo. (c) A simplified sketch of the main section, which turns to follow the SW margin of the murtoo between 30 and 40 m. The murtoo body (Unit 2) in yellow. (d) Dip directions of sand beds and current ripples, and clast fabrics (n = 25) about 25 m from the murtoo tip showing divergent flow pattern. (e) The NNE side of the trench, with boulders concentrated between 6 and 14 m distance (see Figure 6c). Note the size of the largest boulders (<1.0 m in diameter) in the sediment pile.

of the sieve diameter from 50 boulders from Units 1 and 2, the average boulder size is 0.4 m and only 16% of boulders are 0.5–1.0 m in size. The overall paleoflow pattern of the murtoo head is lobe-shaped, as indicated by the dip of inclined and better preserved sand beds, current ripples and trough-shaped sets (Figure 6d).

4.2.3 | Depositional unit 3

Unit 3 is mostly composed of loose, massive/matrix-supported sandy diamicton with some dispersed cobbles and few boulders (Figures 6c and 7f). The contact with Unit 2 is amalgamated, but partly marked by

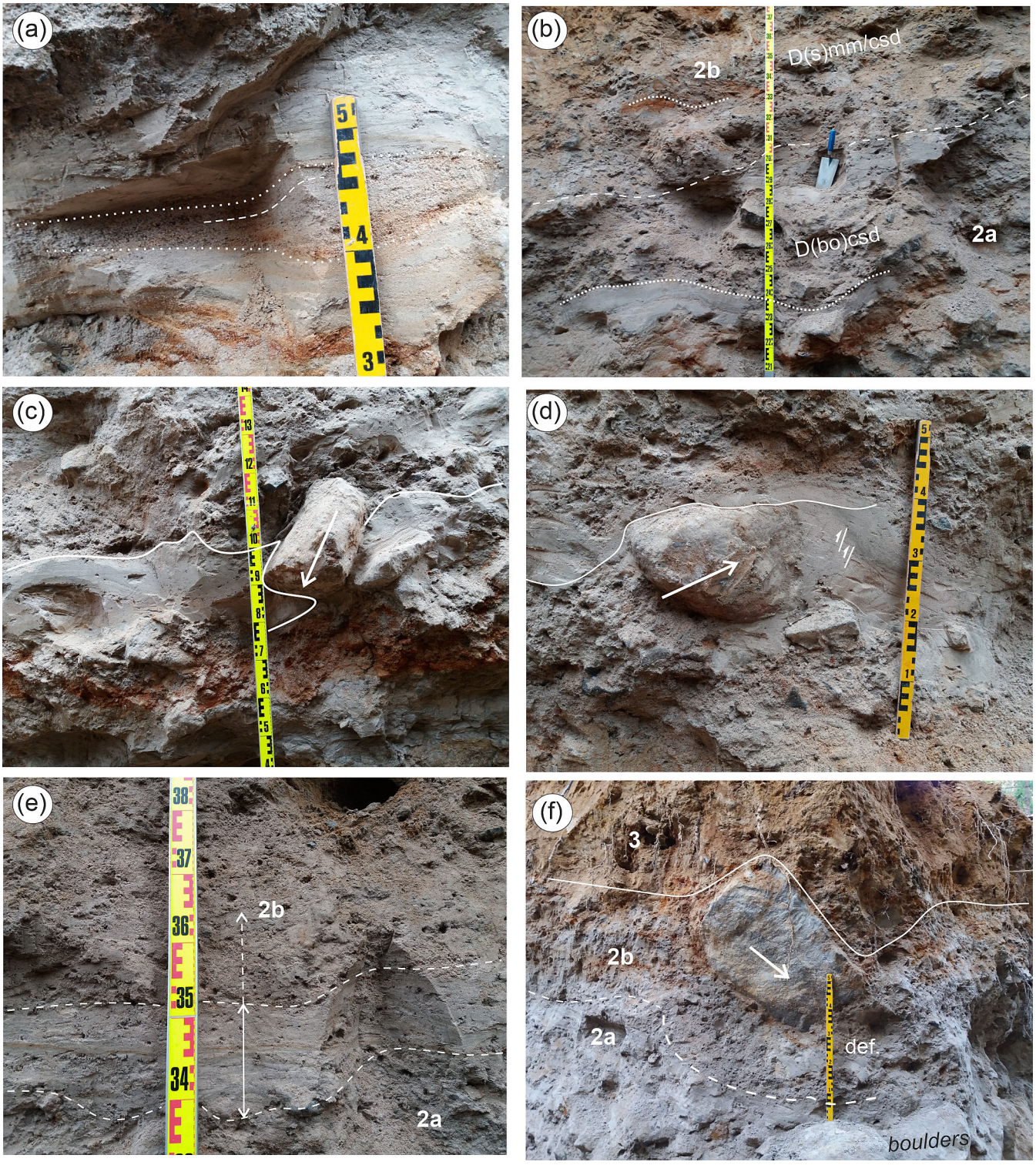

FIGURE 7 Key sedimentary structures from the Kynäsjärvi murtoo. (a) A single current ripple with cross-lamination (dashed line) in Unit 1 outlined by dotted lines (flow oblique towards the left). (b) Distorted remnants or intraclasts of fine-grained sand beds (dotted lines) with deformed lamination in Unit 2 (dashed line indicates the boundary between subunits 2a and 2b). Note the ductile deformation with intense mixing of sands with gravel spotted by pebbles. (c) A cobble cutting through (arrow) the highly deformed sand bed on top of Unit 1 (solid line). (d) A small boulder pushed against the sand bed with small faults. (e) Laterally more continuous, but poorly preserved, muddier laminated/deformed sand bed. It has been mixed into the lower part of subunit 2b (dashed arrow). (f) A large boulder pushed down (arrow) into the murtoo body (subunit 2b) deforming the sediments below and overlain by the sand-rich murtoo mantle (Unit 3).

a non-continuous cobble layer, one clast thick. The unit is disturbed by the forest bed processes with well-developed podsol soil. The murtoo surface exhibits approximately 5 boulders/100 m^2 west of the trench.

4.3 | Kämmäkkä (Kä)

The Kämmäkkä murtoo (Kä 1) was excavated through the low-relief murtoo head about 1.5–2.0 m high (Figure 8). The section is 20 m long

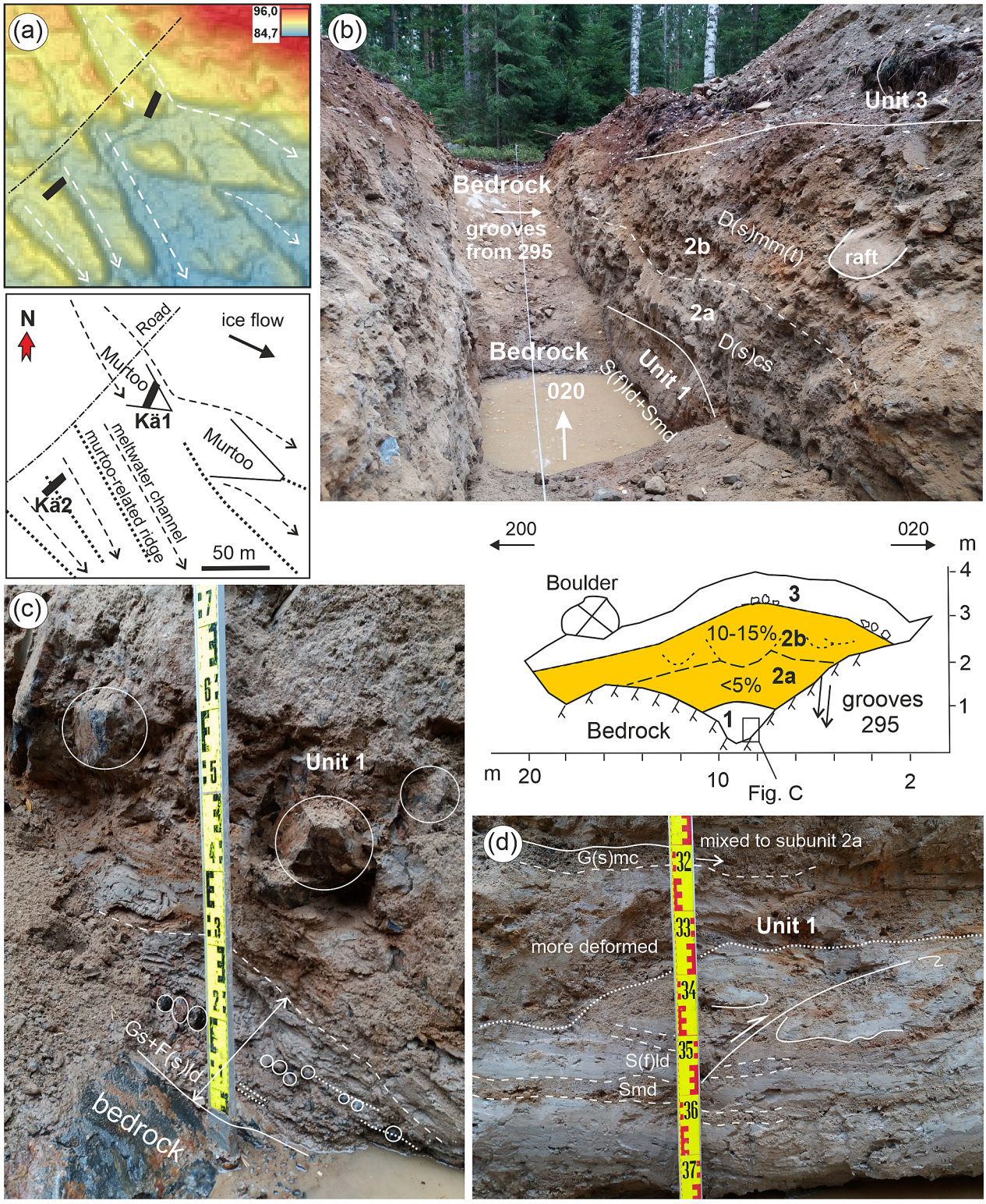

FIGURE 8 The Kämmäkkä murtoo. (a) Location of the trench (Kä1) in relation to murtoo-related ridges (Kä2) and meltwater channels. Colour ramp in m a.s.l. (background map source: LiDAR DEM, © National Land Survey of Finland, 12/2021). (b) A photo towards NNE along the section Kä1 (dashed line indicates the boundary between subunits 2a and 2b) and a simplified sketch of the section with depositional units. The murtoo body (Unit 2) in yellow. Note the bedrock trough filled with groundwater. (c) Lithofacies association directly on the bedrock composed of laminated/thinly bedded granule to fine-pebble gravel interbedded with deformed silt to silty sand laminations (Gs + F(s)ld) representing a distributed drainage system (dashed and dotted lines with circled pebbles) before the deposition of Unit 1 (cobble clasts circled). (d) Deformed Unit 1 with a small thrust fault (arrow + solid line). Dashed lines indicate bed boundaries and dotted line the lower contact of homogeneously deformed sediments.

with a 3-m wide and 1.5-m deep bedrock trough in the centre of the murtoo without intervening basal till (Figure 8b,c). The bedrock is ice-abraded with grooves oriented in the direction of 295°, which corresponds to the local ice flow towards ESE. The thickness of murtoo sediment is about 2.0–3.5 m. An additional pit (Kä2) was excavated through a small murtoo-related ridge to enable a comparison of the internal structure and lithology (Ojala et al., 2021). Excavated murtoo sediments are divided into three architectural/depositional units.

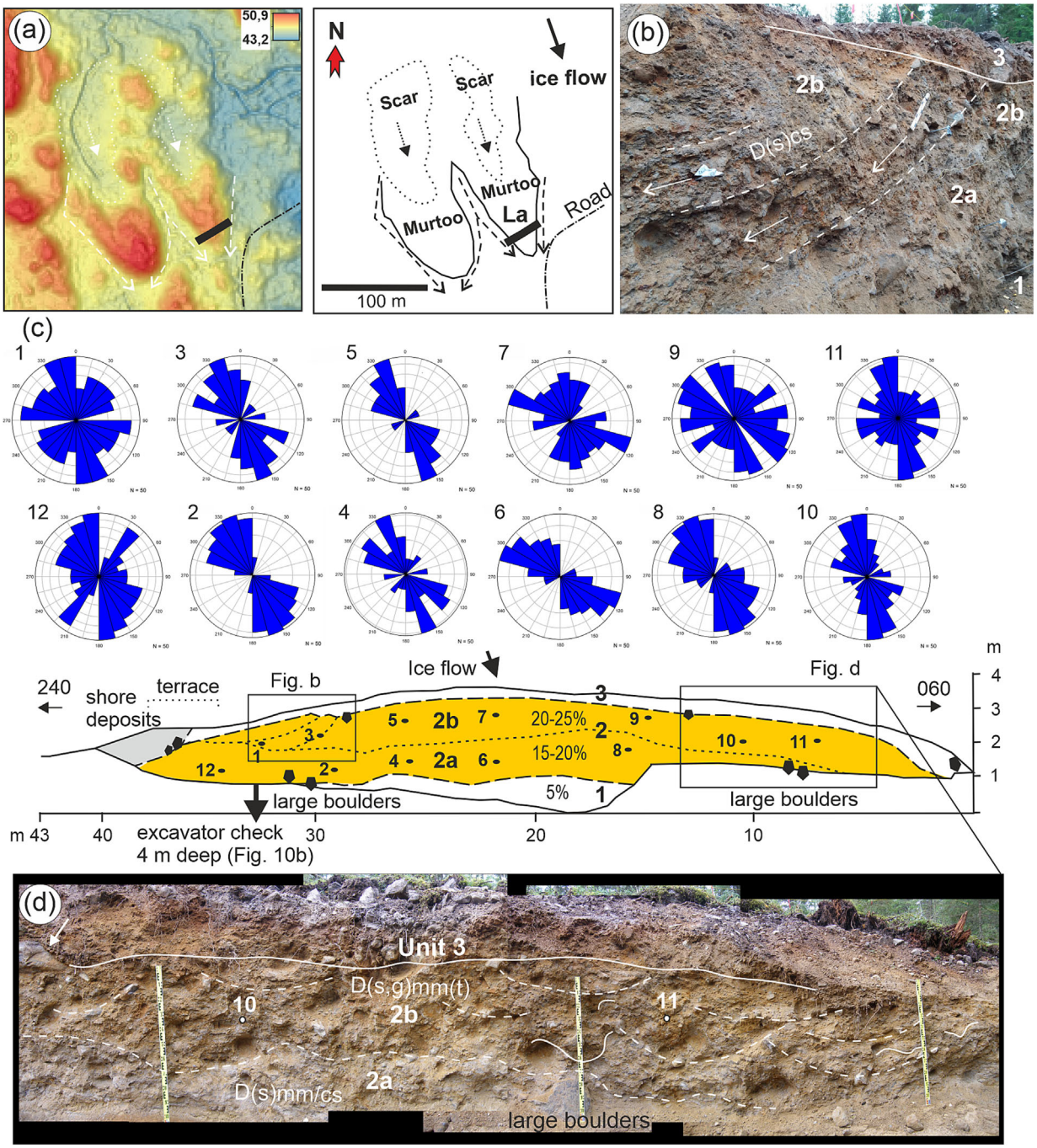

FIGURE 9 The Laihia murtoo. (a) Location of the trench (La) in relation to adjacent murtoos and their proximal scars and lateral meltwater channels. Colour ramp in m a.s.l. (background map source: LiDAR DEM, © National Land Survey of Finland, 12/2021). (b) A large marginal trough in subunit 2b within the SW side of the murtoo composed of sandy, crudely stratified diamicton (dashed lines indicate bed boundaries). (c) A simplified sketch of the section with macrofabric measurements (n = 50), stone percentages and depositional units. The murtoo body (Unit 2) in yellow. Macrofabrics show strong orientation in the middle (except for numbers 7 and 9 measured next to boulder and a diamicton trough) and a more divergent pattern along the margins. (d) Distinct subunits 2a and 2b (separated by the dashed line) within the NE margin of the murtoo including macrofabrics 10 and 11. Note the crude trough-shaped sets (dashed lines) becoming slightly more clearly visible towards the margin of the murtoo in more gravelly subunit 2b. Solid lines indicate slight ductile deformation. The white arrow indicates a ploughed boulder overlain by crude fissility in contact between units 2 and 3. Photo towards the proximal part of the murtoo.

4.3.1 | Depositional unit 1

Unit 1 is confined to the bedrock trough. The lowest part is composed of a 15-cm thick facies association that is conformable to the bedrock surface, consisting of silt or silty sand laminations (deformed) interbedded with laminated/thinly bedded granule to fine-pebble gravel (Figure 8b,c). These sediments are overlain by nearly horizontal beds of deformed, laminated silty fine sand (3–10 cm thick) interbedded with deformed, massive, medium to coarse-grained sand beds (1–2 cm thick) (Figure 8d). Unit 1 contains outsized clasts and includes a 0.5-m long thrust fault (Figure 8d), overlain by more homogeneously deformed sediment. The unit is eroded at the top, above which was

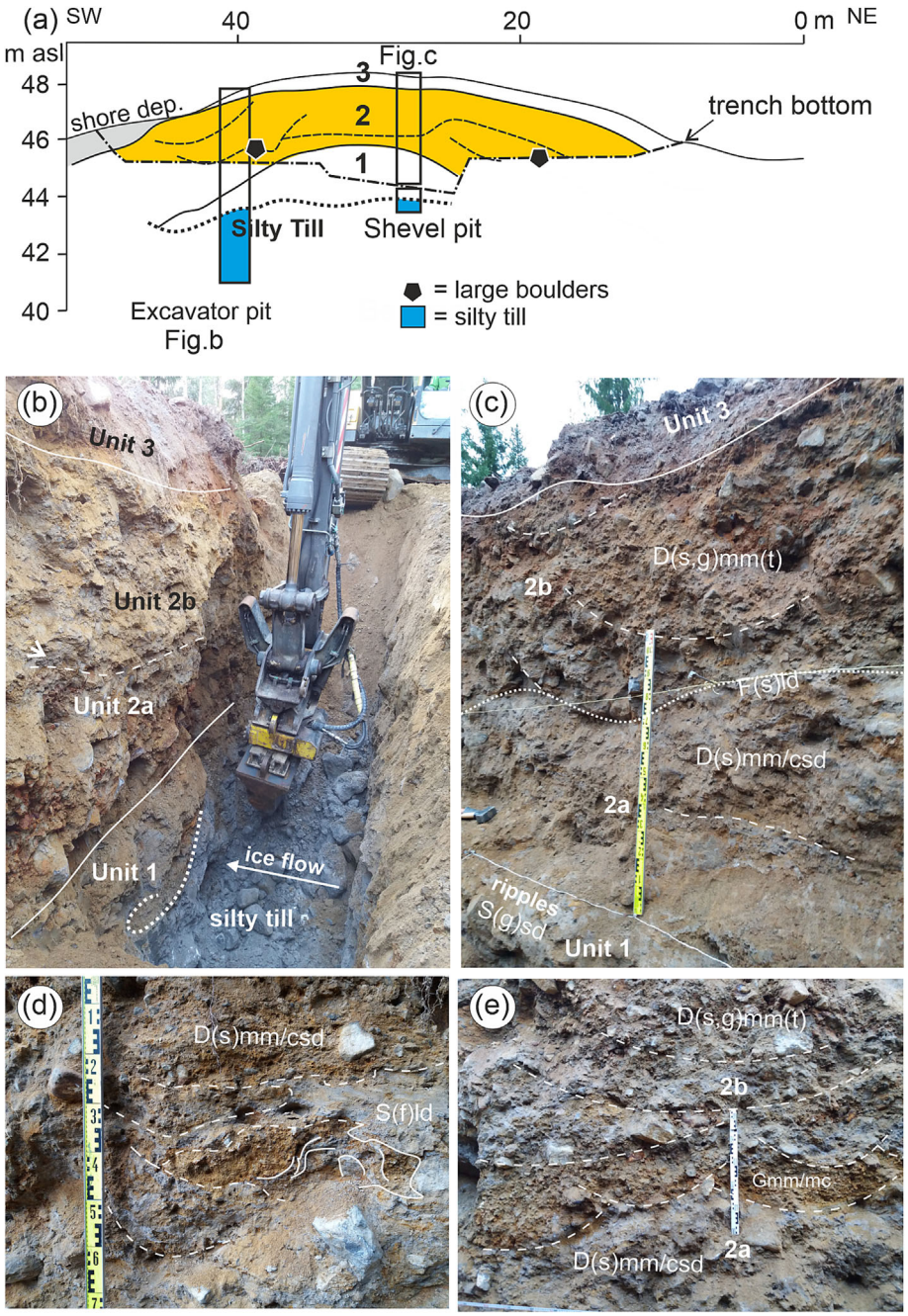

FIGURE 10 The Laihia murtoo. (a) The excavated section in relation to test pits dug down to silty till. Main murtoo body (Unit 2) in yellow. Note the location of figures b and c. (b) Dark grey silty till below murtoo sediments (Units 1–3). Dashed line separates subunits 2a and 2b. (c) Depositional units of the murtoo with a laterally continuous silt-rich bed (F(s)ld) separating subunits 2a and 2b (dotted line). Unit 1 topped by large current ripples. The more gravelly subunit 2b shows crude trough-shaped diamictons with cobble lags (dashed line). (d) A slightly dislocated and deformed silty fine-grained sand (S(f)ld) bed in subunit 2a, forming chaotic streaks in gravels or sandy diamictons (bed boundaries with dashed lines). Signs of ductile deformation above a small boulder (solid lines). (e) Well-defined trough-shaped (dashed lines) diamictons in subunit 2b with the lowermost troughs consisting of massive, partly clast-supported gravels.

deposited a nearly horizontal 5-cm thick bed of massive/clast-supported sandy fine gravel (Figure 8d), indicating increased meltwater flow.

4.3.2 | Depositional unit 2

The lower part of Unit 2 (subunit 2a) is composed of sandy, crudely stratified diamicton with a matrix consisting of fine- to medium-grained sand (Figure 8b). The diamicton includes remnants of silty fine-grained sand beds and pebbly gravel beds. It also contains some out-sized cobble–small boulder clasts (stoniness <5%) that have been pushed down within sediment pockets intruding into the underlying sediments.

Subunit 2b is clearly stonier and composed of sandy massive/matrix-supported diamicton with trough-shaped sets. These sets have weak bottom lags and beds (1–2 cm thick) of deformed silty fine sand conformable to the troughs, as well as occasional sand rafts (Figure 8b). The lower contacts of the troughs are either amalgamated or sharp/erosional in association with more gravelly sets.

4.3.3 | Depositional unit 3

Unit 3 is composed of a loose and poorly sorted sandy massive/matrix-supported diamicton with boulders, and is mostly disturbed by forest bed processes. The diamicton is partly underlain by a poorly preserved layer of stratified fine- to medium-grained sand. The lower

contact with Unit 2 is amalgamated, displaying crude gravel layers, one clast thick. The density of surface boulders is about 5 boulders/100 m^2.

4.4 | Laihia (La)

At Laihia, a 40-m long and 2.0- to 2.5-m high section was excavated through a chevron type murtoo (cf. Ojala et al., 2021, Figure 9a). The SW part of the trench was excavated 4 m deeper, revealing a 2.0-m thick, clearly differently coloured, grey and silty massive/matrix-supported diamicton (till) (Figure 10a,b). The silty diamicton was also detected in a shovel pit dug into the central part of the trench. It contains approximately 26% silt and 4% clay. The murtoo deposits are 4–5 m thick. Excavated murtoo sediments are divided into three architectural/depositional units. A small terrace with well-sorted coarse sands indicates erosion and deposition by shore processes along the SW margin of the murtoo (Figure 9c).

4.4.1 | Depositional unit 1

Unit 1 is gently arched and about 2 m thick and 30 m wide (Figures 9c and 10a). It is mainly composed of stratified, moderately sorted medium- to coarse-grained sand spotted by granules and small pebbles. It displays slight deformation, containing grey streaks of fine- to medium-grained sands, occasional current ripples, as well as fine gravel patches and occasional cobbles. The composition of sands is similar to the matrix of the underlying silty diamicton.

4.4.2 | Depositional unit 2

With a partly sharp/erosional or an amalgamated contact to Unit 1, subunit 2a is composed of slightly compact, sandy massive/matrix-supported to crudely stratified/deformed diamicton with weak trough-shaped sets and pebble-cobble lags (Figure 10c). The diamictons include greyish streaks of fine sand (1–3 cm thick) with deformed lamination (Figure 10d), patches of granule-rich very coarse sand and open-work gravel lenses. The largest boulders, up to 0.7 m in diameter, occur approximately 8 m from the murtoo margins. Subunit 2a is topped by a partly preserved 5- to 30-cm thick, deformed greyish silt to silty very fine sand horizon (Figure 10c), containing 55% mud and 6.6% clay.

Subunit 2b is less compact and composed of sandy and gravelly, massive/matrix-supported diamicton with some 0.4–0.5 m boulders (Figures 9d and 10c) or massive- to clast-supported pebble gravel with well-defined trough-shaped sets (Figure 10e). The subunit also contains open-work gravel patches and open-work tube-like structures about 30–40 cm high and 0.5 m wide. The SW margin of subunit 2b shows trough-shaped sets composed of crudely stratified sandy diamicton with few crude cobble layers (Figure 9b). Subunit 2b within the NE margin reveals crude trough-shaped sets with some streaks and rafts of silty fine sands, as well as signs of ductile deformation (Figure 9d). The contact with underlying subunit 2a is amalgamated and slightly undulating.

The diamictons in Unit 2 contain only 0.7–1.4% clay and 3.8–9.5% mud. The clasts in Units 1 and 2 are dominantly subangular to subrounded. Clast fabrics in Unit 2 show a strong flow-parallel alignment towards the murtoo tip in the middle part of the murtoo, whereas clast fabrics become more divergent closer to the murtoo margins (Figure 9c). However, clast fabrics in the middle part (fabrics 7 and 9) may also show a less preferred orientation when measured close to boulders or trough margins (Figure 9c).

4.4.3 | Depositional unit 3

Unit 3 is composed of a loose, sandy and poorly sorted massive/matrix-supported diamicton with boulders (Figure 9c,d). It is about 0.5 m thick and the lower contact with Unit 2 is sharp or amalgamated. The contact contains some boulders that are slightly pressed down into Unit 2 and overlain by sediment showing a crude fissility. In places, a poorly preserved, stratified, medium- to coarse-grained sand layer covers subunit 2b. It displays intrusions and mixing into the overlying massive diamicton. The density of surface boulders is approximately 5 boulders/100 m^2, but the chevron limbs are more bouldery.

4.5 | Mikkeli (Mi)

At Mikkeli, a 37-m long section (K2) was excavated through a 3.0- to 3.5-m high murtoo with clear sharp tip (Figure 11). Three supplementary pits (K3, Tk1 and Tk2, Figure 11) 3- to 4-m-deep were excavated down into the ice-abraded bedrock with grooves (Tk1), indicating ice flow from 320 to 325°. This direction deviates slightly from the local orientation of drumlins and striations (335–340°). The bedrock beneath the murtoo dips about 4 m from the proximal part (Pit K3) towards the front of the murtoo tip (Pit Tk2) (Figure 11d). The excavated murtoo overlaps the neighbouring murtoo as shown by the LiDAR DEM (Figure 11a). Excavated murtoo sediments are divided into three architectural/depositional units.

4.5.1 | Depositional unit 1

The bedrock beneath the front of the murtoo (Pits Tk1 and Tk2) contains an approximately 2-m deep trough filled with wet silt/silty fine sand that is massive to weakly laminated/deformed with some pebbles and occasional cobbles (Unit 1, Figure 11c,d). A shovel pit in the main section (K2) also reveals 0.7 m of wet massive silt with small pebbles (Figure 11c). The samples from the silt-rich beds contain 87.7–91.2% silt, 4.0–6.6% clay and 4.8–5.7% sand.

The lowest 15-cm thick bed in Pit Tk1 directly on the bedrock displays a bed composed of interlaminated silt and medium- to coarse-grained sand with small pebbles. Interestingly, this bed shows the same facies association as in the narrow bedrock trough of the Kämmäkkä murtoo, also overlain by silt-rich sediments. The top of Unit 1b is composed of broadly arched and 32-m wide silty fine- to medium-grained sand. It contains deformed lamination with a crude upward coarsening and is spotted with granules, pebbles and a few cobbles (Figures 11c and 12a).

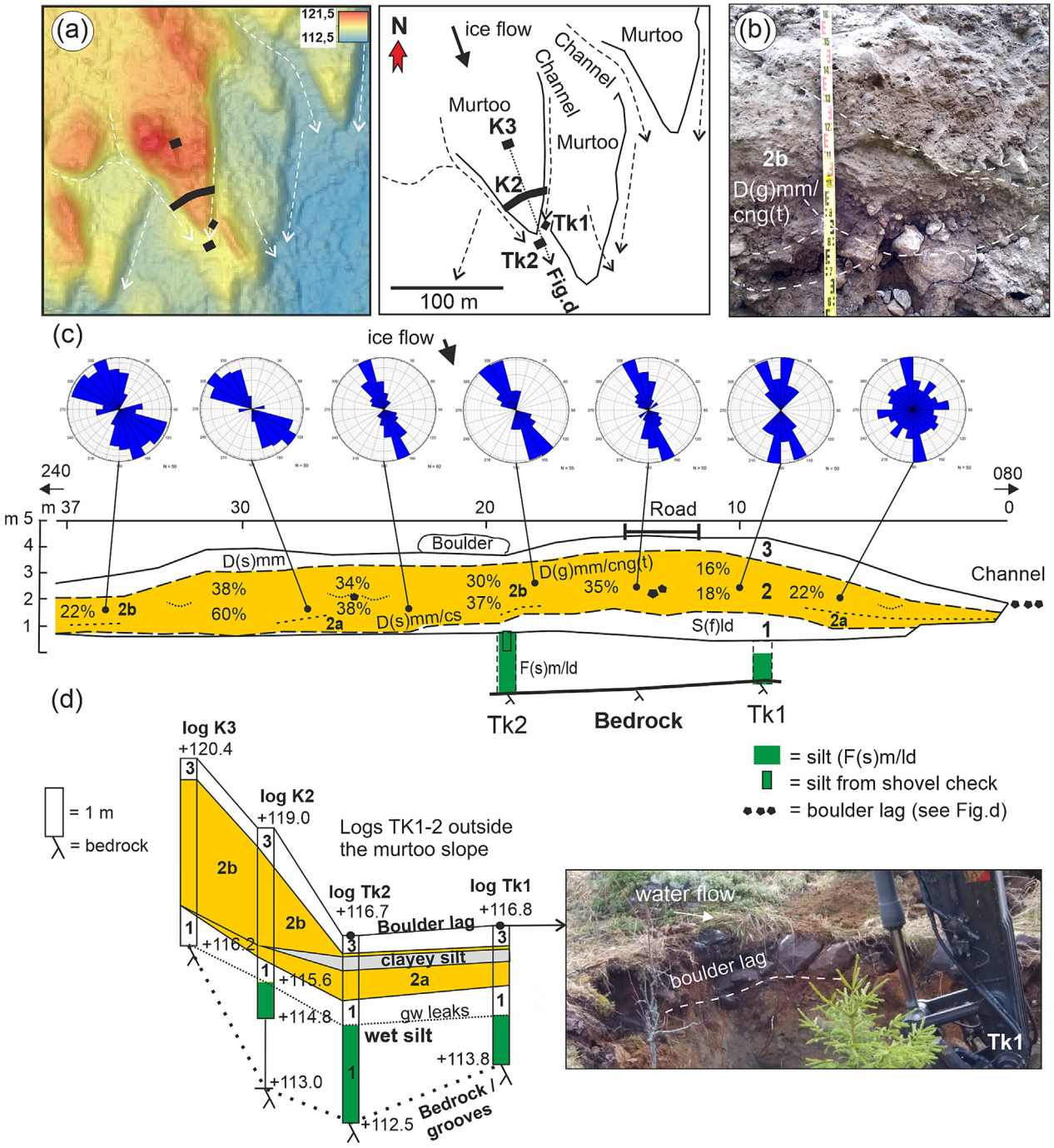

FIGURE 11 The Mikkeli murtoo. (a) Location of the main trench (K2) in relation to supplementary pits Tk1-2 and K3, adjacent murtoos and meltwater channels. Colour ramp in m a.s.l. (background map source: LiDAR DEM, © National Land Survey of Finland, 12/2021). (b) Massive clast-supported/open-work gravels with normal grading on the bottom of troughs and changing upwards to massive/matrix-supported diamictons in the proximal Pit K3. Dashed lines indicate set boundaries. (c) A simplified sketch of the section K2 with macrofabric measurements (n = 50), stone percentages, depositional units and relative position of Pits Tk1-2 located outside the murtoo. Unit 2 in yellow. Macrofabrics show strong orientation in the middle and a more divergent pattern along the margins. (d) Simplified sediment logs showing the relationship between the bedrock surface and the depositional units from the proximal Pit K3 to Pit Tk2 in front of the murtoo tip. Pit Tk1 is located lateral to the murtoo tip. Altitudes in meters a.s.l. measured with an excavator-mounted GPS device. Photo at right shows the boulder lag of the channel between murtoos (see Fig. a).

4.5.2 | Depositional unit 2

The lower part of Unit 2 is composed of sandy massive/matrix-supported to crudely-stratified diamicton with deformed patches of sand (subunit 2a, Figure 12). The eastern side of subunit 2a is topped by a massive bed of mud (27.3% clay, 71.1% silt, 1.6% sand), approximately 20–25 cm thick (Figures 11d and 12b). It is partly mixed into subunit 2b, but mostly eroded within the main section (K2). The mud layer was also found in Pits Tk1 and Tk2 in front of the murtoo (Figure 11d).

Subunit 2b is composed of gravelly massive/matrix- to clast-supported diamicton that occurs as several trough-shaped sets with

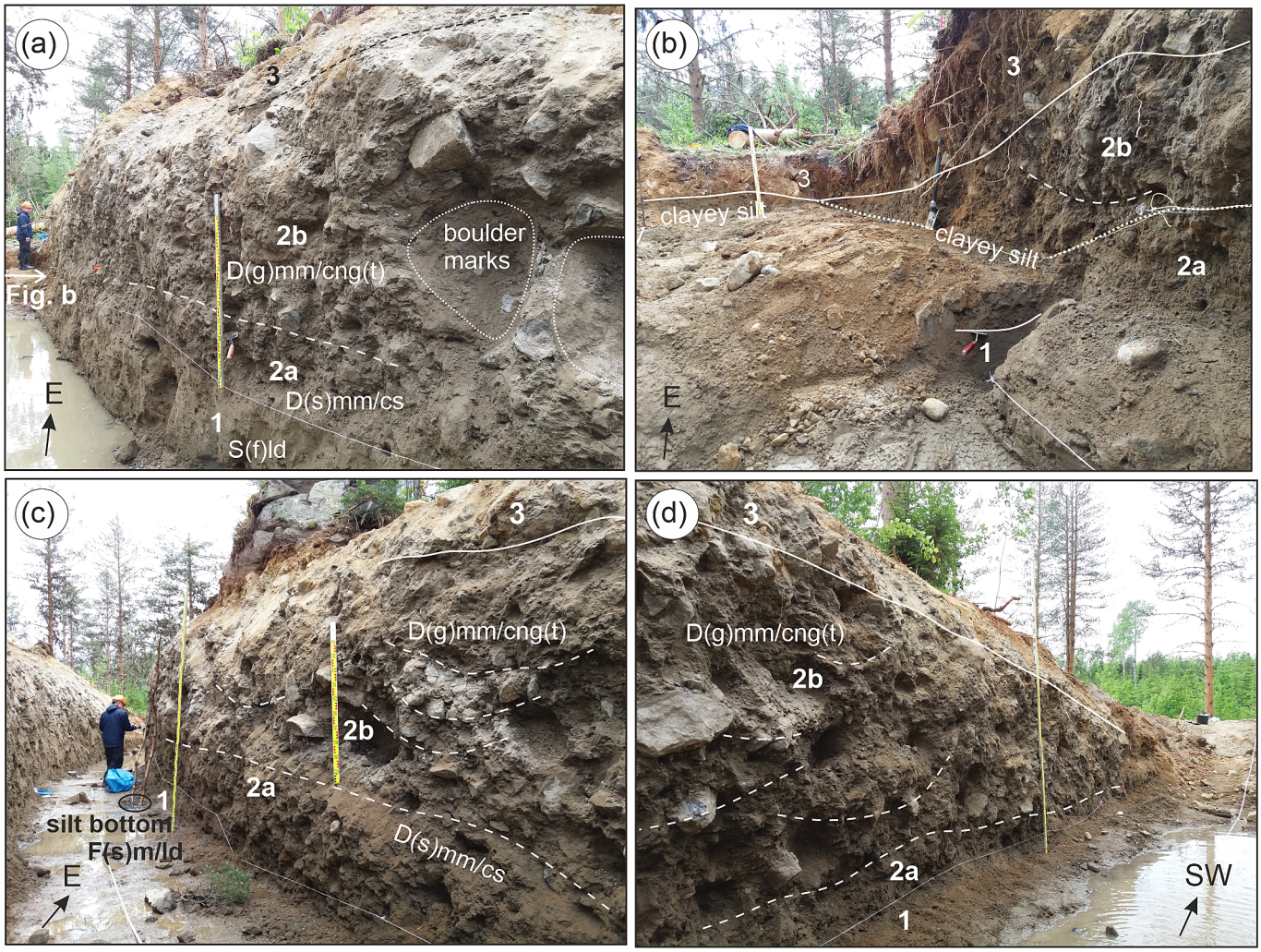

FIGURE 12 Depositional units in the central and marginal parts of the Mikkeli murtoo in the section K2. (a) Upwards coarsening of Units 1 and 2 at the eastern end of the section. Dashed line indicates the boundary between subunits 2a and 2b. (b) The eastern end of the section, revealing a marginally preserved clayey silt bed that separates subunits 2a and 2b (dotted line). (c) Large trough-shaped diamictons (dashed lines) with basal massive/clast-supported or open-work gravel with normal grading indicative of hyper-concentrated flows. Subunits 2a and 2b separated by a dashed line. (d) the SW margin of the murtoo with crude trough-shaped diamictons (dashed lines) in subunit 2b. The subunits separated by dashed line). All images show the pit bottom in wet silt-rich sediments (F(s)m/ld), forming the base of the murtoo on the bedrock as shown by Pits Tk1-2 in Figure 11c.

cobble–boulder lags (Figure 12). The clay content is 1.0–1.3% and the size of the largest boulders approximately 0.5 m. The base of some troughs contains beds (<30 cm thick) of open-work gravel with coarse-tail normal grading, overlain by massive/matrix-supported diamictons (Figures 11b and 12c). The contacts between troughs are mostly amalgamated. Subunit 2b includes occasional small (5 × 10 cm) patches of fine- to medium-grained sand. The stoniness is high increasing from 16–22% to 35–60% towards the west where the diamictons display a more clast-supported texture and well-defined troughs that are commonly 0.5 m high and 2–3 m wide (Figure 12c).

The clast fabric measurements from subunit 2b indicate strong clast orientation in the middle of the murtoo parallel to the local ice flow, whereas the murtoo margins show more diverse directions (Figure 11c). The pebble-sized clasts in Units 1 and 2 are mainly angular to subangular, whereas larger clasts are mainly subangular to subrounded. Importantly, subunit 2b is clearly restricted to the triangular shape of the murtoo with steep slopes.

4.5.3 | Depositional unit 3

Unit 3 has an amalgamated contact to subunit 2b, including a crude cobble-small boulder layer, one clast thick. It is composed of a loose, massive/matrix-supported diamicton with boulders and includes thin beds of open-work gravel (Figure 12). The murtoo surface has 17–20 boulders/100 m^2. The channel between the overlapping murtoos has a boulder lag with weak imbrication, indicating lateral erosion of Unit 3 (Figure 11d).

4.6 | Sievi (Si)

The excavated murtoo at Sievi forms the head of a composite murtoo, the NE side of which consists of a few small murtoos sharing the same long erosional margin (Figure 13a). A 33-m long trench (Si1) was excavated across the 4-m high murtoo, the tip of which is joined by a small ridge about 1–3 m high and 25 m wide (Figure 13a,b). One

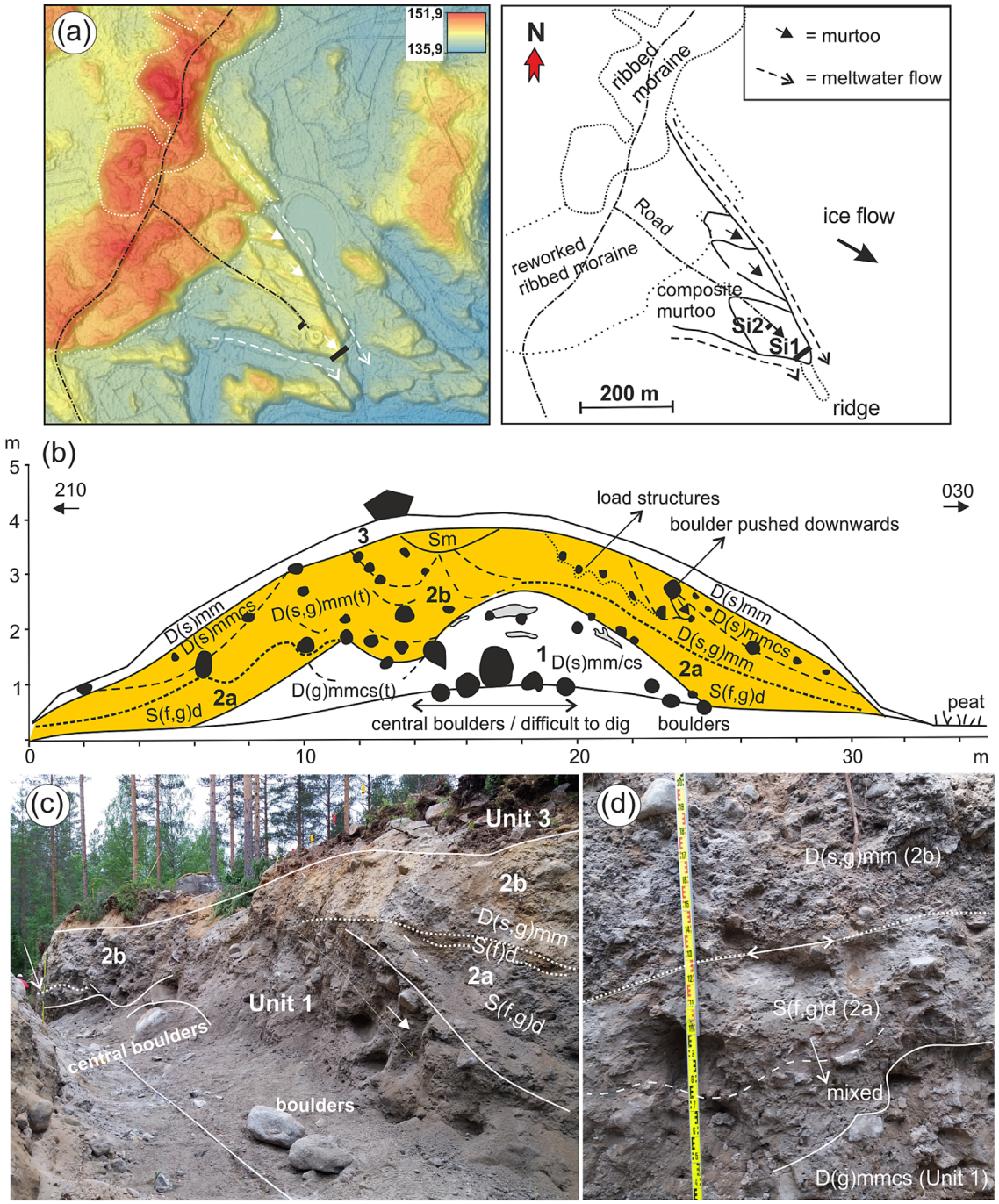

FIGURE 13 The Sievi murtoo. (a) Location of the trench (Si1) and supplementary pit (Si2) in relation to the composite murtoo, ribbed moraine ridge and lateral meltwater channels. Colour ramp in m a.s.l. (background map source: LiDAR DEM, © National Land Survey of Finland, 12/2021). (b) A simplified sketch of the section with depositional units. The murtoo body (Unit 2) in yellow. (c) An arched core of the murtoo (Unit 1). Lithofacies S(f)d with fissile structure forms the boundary between subunits 2a and 2b (dotted lines) (photo towards the west). (d) Subunit 2a mostly consisting of highly deformed silty fine-grained sand (S(f,g)d) that is mixed with underlying gravelly sediments (dashed line) within the SW margin of the murtoo. Subunit 2a is partly mixed (dotted line) into the massive diamicton in subunit 2b.

supplementary 2.5-m deep test pit (Si2) was excavated until the groundwater level in the proximal part of the murtoo (Figure 13a). The Sievi murtoo has the most complex structure of all the murtoos studied here, but can also be divided into three architectural/depositional units.

4.6.1 | Depositional unit 1

The bottom of the section reveals an arched central cluster of boulders (the largest about 1.0 m in diameter) draped by massive silty sand (Figure 13b). Unit 1 is mostly composed of highly sandy, massive/

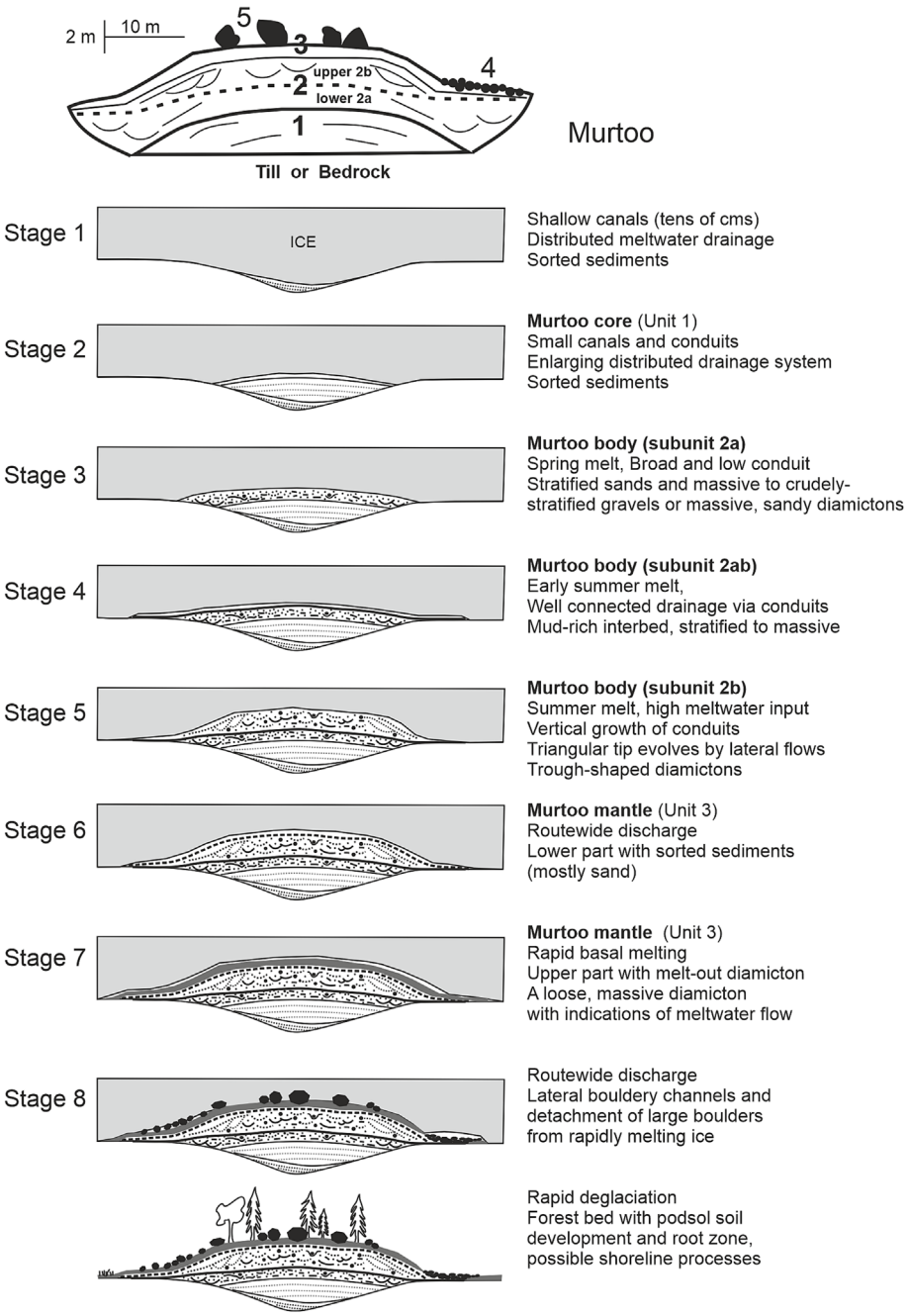

FIGURE 14 Murtoo architectural/depositional units and suggested stages of murtoo formation.

matrix-supported to crudely stratified diamicton, containing only 1.0% clay and 5.0% silt, and forming an arched core of the murtoo (Figure 13b,c). The unit includes rafts of fine-grained sand and remnant sand beds (5–20 cm thick) with deformed lamination, as well as 2- to 3-cm thick lenses of open-work gravel. Unit 1 can probably be associated with the small ridge that continues down flow from the murtoo tip (Figure 13a).

4.6.2 | Depositional unit 2

Unit 1 is covered by a deformed sandy bed (subunit 2a) spotted by pebbles. It is 0.5–1.0 m thick with an amalgamated contact to Unit 1 (Figure 13b,c) and includes rafts of clayey silt. The subunit is topped by an approximately 10- to 15-cm thick layer of silty very fine sand with fissile structure and some granules to small pebbles (Figure 13c). This layer becomes mostly eroded towards the SW.

Subunit 2b consists of sandy and gravelly, massive/matrix-supported diamicton with 1.0% clay and 5.0% silt. However, the lowest and the most poorly sorted massive diamicton, in contact with subunit 2a, contains 2.4% clay and 12.3% silt (Figure 13d). The subunit includes occasional rafts of fine sand and crude cobble lags, forming trough-shaped sets, especially in the upper part of the subunit. The largest clasts are 0.5–1.0 m in diameter and they are in places coated by open-work gravel that also occurs as occasional 20- to 30-cm high and 30-cm wide patches.

The NE margin of subunit 2b contains massive load structures approximately 0.5 m in height and width with large cobbles or small boulders inside them (Figure 13b). These structures appear to be oriented linearly in the direction of 110–290°, corresponding to nearby 120–300° striations. They are laterally in contact with a large push structure associated with one boulder (0.7 m in diameter) that has compacted sandy gravel below it (Figure 13b).

Finally, both margins of the murtoo became eroded by deposition of trough-shaped sets composed of strikingly loose, sandy and stony (15–20%), massive/matrix-supported to crudely stratified diamicton (Figure 13b). The clasts are visually more angular than elsewhere in the section. The largest clasts are 0.5–0.6 m in diameter.

The pebble-sized clasts in Units 1 and 2 are dominantly angular to subangular and the larger clasts are mainly subangular to subrounded. Section Si2 in the proximal part of the murtoo reveals a sediment structure similar to the middle part of the main section, suggesting the continuation of the arched core.

4.6.3 | Depositional unit 3

Unit 3 is about 0.5 m thick and composed of a loose, sandy massive/matrix-supported diamicton with boulders (Figure 13c). The contact to subunit 2b is amalgamated but contains a discontinuous clast layer, one clast thick. The density of surface boulders is 6–10/100 m^2.

5 | INTERPRETATION OF DEPOSITIONAL UNITS AND THEIR SEDIMENTS

All excavated murtoos show similar sedimentological characteristics that have been divided into three main architectural/depositional units: Unit 1 (the core), Unit 2 (the murtoo body) and Unit 3 (the murtoo mantle) (Figure 14, Table 4). There are some variations in the composition of the units between the sites, but characteristically, all of them reveal diamicton in trough-shaped sets in the upper part of the murtoo body. All sites exhibit poor rounding of clasts, ranging between angular to subrounded (dominantly subangular), which indicates short transport distances within the subglacial system. The Kullaa and Kynäsjärvi sites record the highest quantity of angular pebbles but also the most sorted and coarse-grained cores, as well as the best-stratified lower part of the murtoo body. Furthermore, both sites are located within the best-developed meltwater routes of this study, implying that these murtoos show the highest influence of meltwater activity. Thus, the higher number of angular pebbles could be explained by higher erosion rates of the substratum and related short transport distances.

The clay content in diamictons of Units 1 and 2 is between 0.7 and 1.5% (except 2.5% in one diamicton in Sievi, Figure 15), indicating that the clay component of sediment in transport was passing through the subglacial drainage system. The maximum clast size (sieve diameter) in all investigated murtoo sediment is 1.0 m. This is interpreted to indicate the maximum height of the flow space within the subglacial conduit system, whereas the largest boulders remained transported by the ice.

Data from the Geological Survey of Finland (GTK) indicate that regional tills are more homogeneous, have a higher clay and silt content than murtoo bodies (Unit 2), and have boulder sizes exceeding 1.0 m in diameter (S2,S3). Murtoo diamictons are also more sandy and gravelly and contain silty, sandy and gravelly intraclasts (Figure 15). Based on the classification of poorly sorted sediments by Hambrey (1994), the diamictons sampled here could be classified as either poorly sorted gravels or clast-rich sandy diamictons (Figure 15). The till data of GTK from the Kynäsjärvi murtoo field indicate a highly similar composition to the murtoos studied here, whereas tills (mainly hummocky moraine) surrounding the murtoo field have higher mud and clay contents (S3).

TABLE 4 Description and interpretation of the depositional units of murtoos.

Unit	Description	Interpretation
1. Core	Arched, stratified. Sorted sediments with massive silt, laminated silty fine sand, massive medium sand, few current ripples, crudely stratified to massive gravels. Weakly deformed/contorted.	Subglacial small canals and conduits dominated by stream flow. Clay flushed. Rapid deposition of gravels from heterogeneous suspension.
2. Murtoo body	Sandy/gravelly, massive/matrix-supported and crudely stratified diamictons. Trough-shaped sets characteristic for the diamictons in the upper part. Lobate flow directions and marginal channelised diamictons. Loose to moderately compacted. Minimal clay content and sandy matrix. Mainly subangular clasts, boulder-size limited to 1 m. Diamictons intercalated with remnants of deformed/contorted laminated fine to medium sands, some current ripples. Open-work (also with normal-grading) gravel patches and crude clast layers. Spotted pebbly texture and outsized clasts common. Load and push structures and large clasts truncating sand beds. Chaotic fine-grained sandy streaks fracturing diamictons.	Subglacial slurries and hyper-concentrated flows. Silt to sand beds by stream flow. Cyclic deposition due to water pressure fluctuations, short transport distances. Widening broad and low conduit/cavity. Flow space max. 1 m. Entrainment from ice-roof melting. Periodic deformation by ice flow. Lateral meltwater flow eroding the steep margins/tip of murtoos during the deposition of channelised diamictons at the later stage of murtoo body formation.
3. Murtoo mantle	Laminated medium to coarse sand, some gravelly beds (incl. troughs) overlain by loose, poorly sorted diamicton mixed with underlying sands (with intrusions). Some trough-shaped clast layers and weak fissility in places. Forest bed with podsol soil.	Sheet flow deposits followed by rapidly melting ice bottom and concomitant meltwater flow. Clogged conduits. Disturbed by forest bed activity. Eroded by shore terraces in places.
4. Channels	Channel bottom with open-work boulder concentrations (empty spaces up to 0.5–1.0 m deep) or boulder lags.	Meltwater channel erosion after murtoo formation, transition to tunnels?
5. Surface boulders	Boulders up to 3 m in diameter. Boulders concentrated on murtoo surfaces.	Melt-out of large boulders, earlier concentration by ice flow towards the widening conduits.

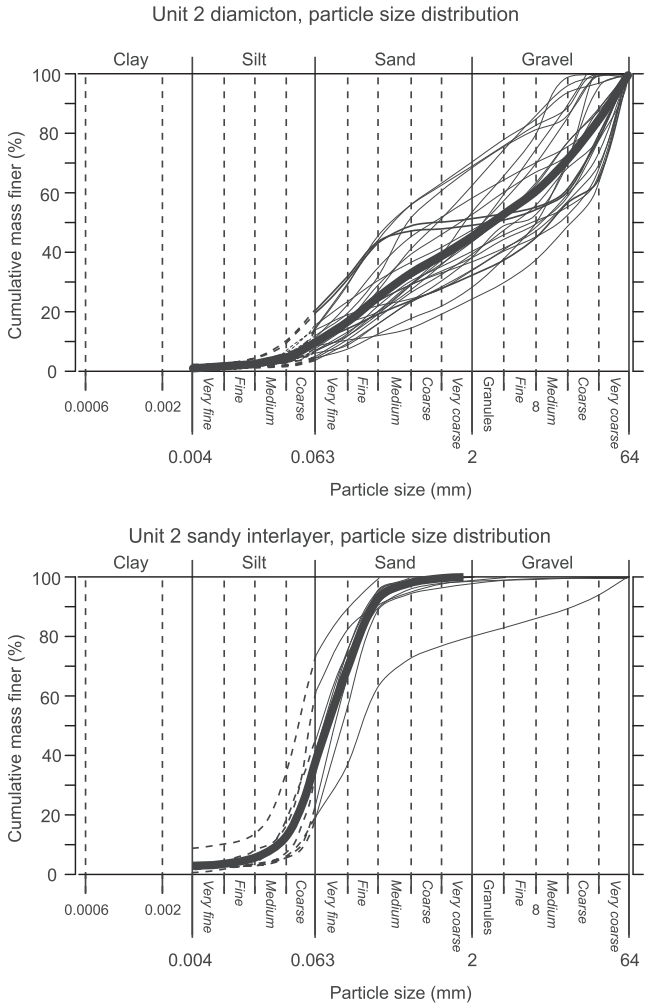

FIGURE 15 The grain-size distribution curves of diamictons (upper) and sandy interlayers (lower) from the murtoo body (unit 2). Diamictons have <1.0–1.5% clay (except <2.5% in one diamicton in Sievi), 3–20% mud, 30–76% gravel, and d_{50} values between medium sand and medium gravel. Sandy interbeds have mainly <5% clay, 18–73% mud, <2.5% gravel, and d_{50} value ranging from coarse silt to fine sand (dominantly very fine sand). The fine-grained bed between units 2a and 2b in Sievi with fissile structure is clearly more poorly sorted compared to other fine-grained units. Thick lines indicate the average grain-size distribution.

5.1 | The core (unit 1)

The broadly arched, better sorted and stratified, and generally less deformed core (1.0–2.5 m thick) of excavated murtoos indicates deposition in a broad and low conduit. At the Kämmäkkä and Mikkeli sites, core sediment deposition was initiated in a narrow bedrock canal. The lowest identical facies associations composed of alternating beds of laminated silt and pebbly fine gravel might represent pulsed flows within a shallow distributed drainage system (Figure 14, stage 1). Massive silts and sands were produced by rapid suspension settling from hyper-concentrated, low-velocity flows, whereas laminated silty sands were deposited from more tranquil stream flows with occasional current ripples indicative of sporadic, slightly increased flow velocities.

Massive gravels indicate pulses of higher flow velocities and can be interpreted to record meltwater flow along the growing conduit or tunnel walls (Brennand, 1994; Shreve, 1972) and rapid deposition from heterogeneous suspension (Mäkinen, 2003). Crudely stratified gravels indicate that the largest clasts within the flow were transported as bed load. Amalgamated contacts (similar matrix) indicate closely spaced depositional pulses. According to Collinson & Thompson (1993), gravels with "massive and crude bedding may involve rapidly fluctuating episodes of sedimentation in which the sediment concentration is high, freezing of load takes place and individual events are hard to distinguish." A higher proportion of the coarsest core sediments occur in association with murtoos that reveal central boulder concentrations or bedrock knobs at their base (e.g., Kullaa and Sievi sites). This might indicate that conduit development was associated with reworking of existing till ridges or with cavities on the distal side of bedrock protrusions.

The overall weak or partial periodic deformation of Unit 1 indicates limited conduit closure by the overriding ice. However, the fine-grained core in Kämmäkkä is interpreted to show upwards increasing deformation in the small bedrock trough just before the widening of the conduit. The scattered small pebbles and out-sized clasts were probably entrained from the melting ice roof, creating the common spotted texture, especially in sand-rich beds.

It is difficult to estimate the time frame for core deposition, but the development of the conduit and cavity system before the deposition of the murtoo body (Unit 2) indicates that murtoos formed in an environment where the drainage system gradually enlarged in order to accommodate increased meltwater and sediment flow, however, tunnels did not form (Hooke, 2019).

5.2 | The murtoo body (unit 2)

The murtoo body (1.5–3.0 m thick) consists of subunits 2a and 2b, which are separated by a discontinuous horizon of muddy, clay-rich glaciofluvial sediments (designated here as subunit 2ab), continuing outside the murtoo slopes (Figure 14, stages 3–5). These muddy sediments might be related to suspension-dominated deposition during the quiescence period between the main meltwater events, with effective pressure fluctuating close to zero (Lesemann et al., 2010). Subunit 2a is seen to extend beyond the steep surficial margins of the murtoos, whereas sedimentological data indicate that subunit 2b, suggesting marginal meltwater erosion, is confined to the murtoo morphology. The steep angle of the murtoo margins already developed during the upper murtoo body stage as supported by marginal channelised flows. Higher overburden pressures probably limited the depositional space for subunit 2a in the central part of the murtoo (cf. Hooke, 2019), whereas the lowest margins experienced channelised flows and related deposition of trough-shaped diamictons as shown by the Kullaa murtoo (Ku2).

Subunit 2a records a higher variability in sediment composition; it is usually sandier and has a more stratified structure with frequent interbeds or patches of sand compared with subunit 2b. This is interpreted to indicate a widening of the subglacial conduit over the underlying core (Figure 14, stage 3). In general, dominantly laminated silty sands with occasional ripples were deposited by tranquil stream flows. However, repeated and more powerful pulses of sediment-concentrated flows produced rapidly deposited beds of massive to crudely stratified gravels and massive/matrix-supported sandy diamictons. These beds include rafts, chaotic streaks and dislocated

patches of sand, suggesting erosion and subsequent rapid deposition from these sediment-concentrated flows. Patches of open-work gravel are indicative of deposition by meltwater flow. The bimodal parallel and transverse to flow clast fabric might be explained by flow conditions close to Lawson type III sediment flows (Lawson, 1979). Moreover, the more stratified marginal trough in Kullaa (Ku2) with backflow ripples also provides evidence for turbulent, lateral stream flows during the formation of the lower murtoo body. Sandy beds and diamictons spotted by granules and pebbles, and associated oversized clasts are interpreted as related to the melting of the ice roof. Furthermore, the sediments were periodically (after each depositional event) deformed by ductile deformation, interpreted to be due to shear stresses induced from the overriding ice and coupled to low shear strength due to high porewater pressures (Lesemann et al., 2010; Peterson-Becher & Johnson, 2021).

Boulder concentrations within the murtoo margins might be due to the development of deeper water with higher energy dissipation as well as higher marginal meltwater flow along the margins of a broad and low conduit (Hooke, 2019). Boulder concentrations were probably formed when the conduit was not able to widen further and became filled with sediments.

The dominantly sandy and gravelly, poorly sorted, matrix-supported diamictons, and their common occurrence in trough-shaped sets within the upper part of the murtoo body (subunit 2b), suggests repeated, often channelised flow events of slurries with high sediment-concentrations, in which the viscosity of the flows was controlled by the water content (Menzies, 1989). In places, open-work gravels with normal grading were deposited in channels, overlain by massive diamictons. This indicates settling of the coarsest clasts from suspension during the waning flow within the lower part of hyper-concentrated flows, while smaller grain-sizes remained in turbulent suspension (Pierson, 2005). Tube-like (piped) openwork gravels within diamictons can be explained either as remnants of hyper-concentrated flows or as nearly horizontal structures allowing the evacuation of water under the ice pressure. The stronger clast orientation parallel to flow along the murtoo centre-line suggests uniform shear.

Importantly, the sudden changes in the character of the diamictons in the murtoo section at Kullaa (Ku1, Figure 3c) suggest rapid flow transformation of sediment flows (Lawson, 1981). The often poorly defined troughs and amalgamated contacts refer to close-in-time repeated flow events. Sharp, erosional trough bottoms with some signs of stratification indicate channelised stream flow preceding more sediment-concentrated flows. Crude clast layers one clast thick that often form trough bottoms and marginal low- to medium-angle clast layers probably represent lags from erosional currents (Collinson & Thompson, 1993; Lawson, 1981). Rafts, streaky stratification and dislocated patches of laminated silty sand within the lower parts of the diamictons suggest entrainment of the underlying sediments and shear-induced deformation and mixing by the overriding sediment flow (Phillips, 2006). Marginal troughs with crude stratification and intercalated silty sand stripes are interpreted to indicate rapidly fluctuating flows. The chaotic structure and the most poorly sorted diamictons of the Sievi murtoo might indicate that sediment transport and deposition were somewhat different from the other study sites. This could be explained by their association with remobilisation of ribbed moraine ridges (Vérité et al., 2021).

The vertical distribution of clast sizes is determined by the grain-size distribution in individual slurries. The lack of inverse grading might refer to incremental deposition and aggradation by multiple debris flows "in which a number of momentum transport processes operate involving both solid and fluid forces" (Sohn et al., 1999, p. 112). Furthermore, as stated by Sohn et al. (1999, p.112), it is difficult to categorise sediment flows, "because individual flows may comprise more than one flow type at an instant in time and are subject to a series of flow transformation during transport" (Lawson, 1981). This chaotic process might lead to heterogeneity of the murtoo diamictons, where individual flow events are difficult to separate. The diamicton properties and common occurrence of trough-shaped sets described here suggest sediment flows close to Lawson type III sediment flows. Such sediment flows are associated with flow channelisation, the shear zone encompassing the entire mass with laminar flow and localised temporary turbulence (Lawson, 1979, 1981). Moreover, thinly laminated silty sands in association with diamictons are common and imply meltwater flow over sediment flow surfaces (Lawson, 1981). The flow-parallel clast fabric in diamictons indicates high rates of laminar shear within individual flows (Sohn et al., 1999).

The chaotic deformation of fine-grained laminated sediments and their streaky appearance, larger clasts cutting through the sand beds, the dominant ductile soft-sediment deformation structures, and downward-protruding diamicton pockets (load structures) or injections of mobile debris with larger clasts can all be related to shear stresses induced by overriding ice and related debris flows (Menzies, 1989). The periodic deformation with a lack of apparent dewatering structures lends support to an effective pressure close to zero at the ice–bed contact (Lesemann et al., 2010). The downward protruding diamicton pockets with large clasts are typically located in the upper parts of subunit 2b, implying increased overburden pressure during the final deposition of the murtoo body.

The subunits of murtoo bodies (subunits 2a–2b) separated by muddy glaciofluvial deposits (subunit 2ab) suggest that they were deposited during similar flow variations after the formation of the core (Unit 1). This type of sediment successions can hardly be deposited over several years, but rather during systematic variations in water input. Therefore, we consider that the lower part of the murtoo body (subunit 2a) formed during the spring peak flow event at re-establishment of the subglacial drainage system, leading to rapid widening of the conduit above the core. Later, the muddy interlayer (subunit 2ab) was deposited at lower flow velocities as the drainage system became wider and better connected over the base of the ice (Vérité et al., 2021). The upper part of the murtoo body (subunit 2b) would then been deposited at an even later stage of the meltwater peak originating from increased ice surface melt. Such meltwater would be subglacially distributed within an already well-connected drainage system with rapidly upwards expanding conduits and cavities. Our scenario thus suggests that the murtoo bodies were built during one single melt season with two meltwater peaks upstream of an efficient drainage system (Chandler et al., 2013). However, some spatial and temporal differences in murtoo body development should be expected, depending on how the pressure conditions and meltwater flow velocities change during a melt season.

The dip direction of more well-preserved beds, current and backflow ripples, and trough-shaped diamicton beds with their clast fabrics all together suggest a lobe-shaped or divergent flow pattern within

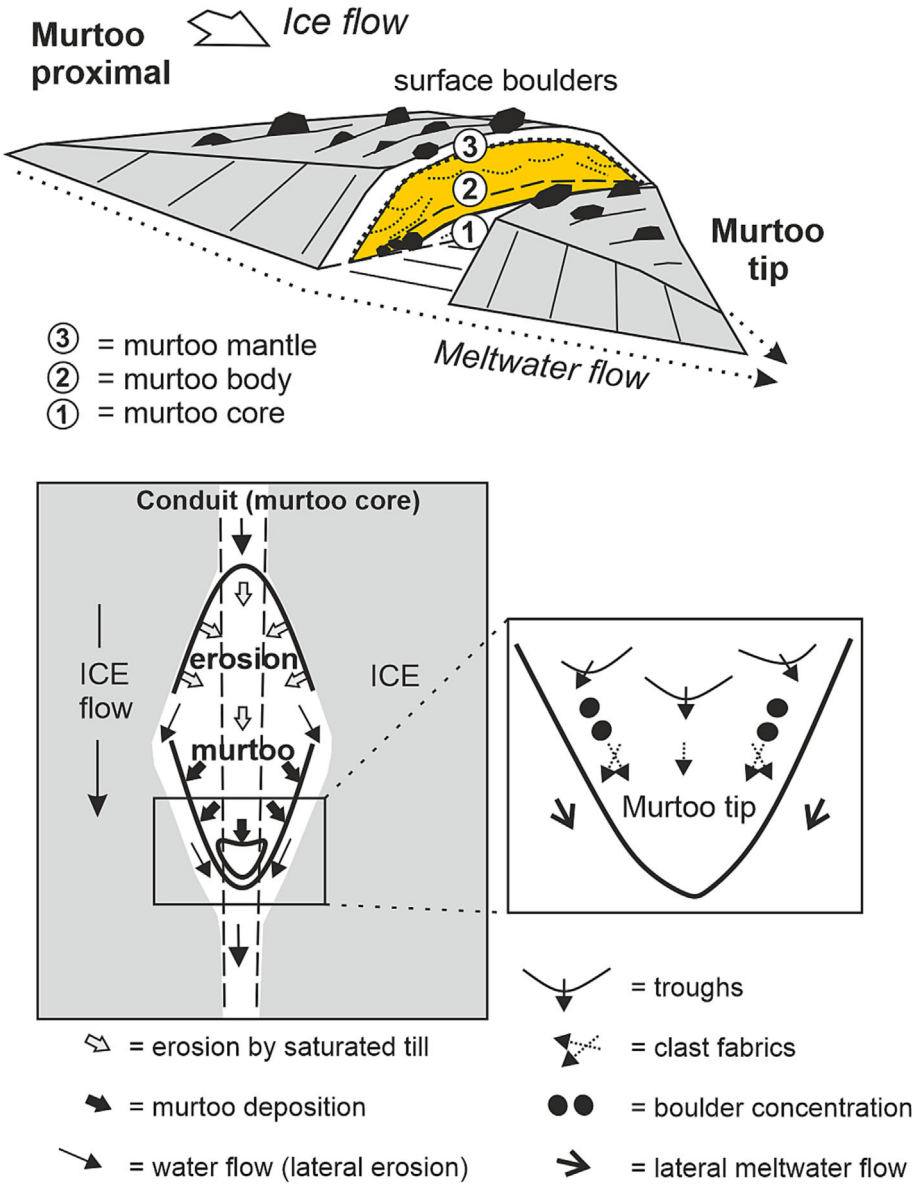

FIGURE 16 A simplified drawing of murtoo with the depositional units and the suggested subglacial depositional environment and flow patterns near the tip on top of the murtoo core (dashed lines). Murtoo cores can develop in a connected subglacial system consisting of canals, conduits or cavities.

the murtoo heads during deposition of murtoo body sediments (Figure 16). This provides evidence that these sediments did not exist prior to their erosion, but were cut to triangular shape by flowing water along the murtoo body margins. The well-defined single murtoos in Laihia and Mikkeli can be used for roughly estimate the volume of the murtoo body sediments (Unit 2), as the topography of the base of the murtoo body can be more reliably estimated at these two sites. Based on the excavations, we estimate that the average murtoo body thicknesses are about 2 m, and the area of each murtoo is about 4,000 m^2. This gives a sediment volume of about 8,000 m^3.

5.3 | The murtoo mantle (Unit 3)

Much of the original sedimentological characteristics of Unit 3 have been altered or erased during later soil forming processes (podsol) and frost activity in these quite thin, uppermost sediments. In spite of this, the Unit 3 diamicton often show a weak stratification and have associated clast horizons (sometimes trough shaped) and interbedded openwork pebble gravel beds, suggesting influence of subglacial water flow also after the formation of the murtoo body (Figure 14, stages 6–7). The poorly preserved arched beds of sorted and stratified sediments (mostly medium and coarse-grained sands) between Units 2 and 3, indicate that murtoo body formation (Unit 2) was followed by diminished stream flow velocities over the whole murtoo. Moreover, the Laihia murtoo clearly shows how these sorted sediments intrude and mix into the overlying diamicton (Unit 3). This might partly explain the common sandy character of Unit 3.

At places the contact between Units 2 and 3 includes ploughed-in boulders, at which the diamicton conformably overlying that contact often reveal a weak fissility, which we relate to shearing of the ice flow (Piotrowski et al., 2001). Importantly, the murtoo mantle (Unit 3) is not only confined to murtoos, but also drapes adjacent murtoo-related ridges (e.g., in Kullaa, Kämmäkkä and Mikkeli), indicating deposition over a wider area of the ice bed.

In a late stage, meltwater channels, up to 0.5–1.0 m deep, eroded the lower part of the murtoo margin, producing open-framework boulder infills (Figure 14, stage 8). Moreover, the murtoo mantle became covered by large boulders (usually 5–20 boulders/100 m^2) deposited from the rapidly melting ice bed interface (Figure 14, stage 8). In places, the murtoo mantle became eroded by shoreline

processes, forming low terraces with downslope, well-sorted sands where murtoos after deglaciation were in subaquatic setting.

6 | DISCUSSION

6.1 | Depositional units and sedimentology of murtoos

Recently, Vérité et al. (2021) interpreted murtoos of the FIS to be associated with a bedform continuum produced by the progressive remobilisation of ribbed moraine due to recurrence of flooding events and ice–bed recoupling. However, they also stated that murtoos do not necessarily form from the transformation of ribbed moraines (cf. Ahokangas et al., 2021; Ojala et al., 2019; Peterson et al., 2017). Moreover, some murtoo-type landforms from northern Finland have been interpreted as V-shaped subglacial mass-flow sediments related to glacially induced palaeoearthquakes and the subsequent subglacial flooding (Sutinen et al., 2021). Peterson-Becher & Johnson (2021) proposed that the subglacial environment of murtoo formation "is within the distributed system where the bed receives meltwater from repeated influxes of supraglacially derived meltwater."

The fact that each murtoo has a stratified core with sorted sediments, sometimes interbedded with diamictons, interpreted as deposited from subglacial slurry flows, suggests initial deposition in a network of low canals or conduits and cavities with fluctuating and variable stream flows (Figure 16). This type of environment suggests formation of murtoo fields within a zone of wet/warm-based conditions along the ice/bed interface and under high overburden pressure. As shown by the sedimentological evidence from our sections, murtoo sediment deposition is characterised by rapid mobilisation of water-saturated sediment and transformation into sediment-concentrated flows within channels or canals incised both down into basal sediment and up into the ice (Eyles, 2006; Nienow et al., 2017).

It is evident that a distributed/linked cavity system versus tunnels forms the end members of subglacial drainage patterns (Hooke, 2019). Therefore, the depositional environment of murtoos, preceded by deposition of murtoo cores within a widening conduit, probably relates to a semi-efficient transitional system in a high-pressure environment not recognised before (Figure 16, cf. Fudge et al., 2008). The proposed semi-efficient drainage system responsible for murtoo formation is suggested to have occurred 40–60 km from the ice margin (cf. Bartholomew et al., 2011; Chandler et al., 2013; Greenwood et al., 2016; Hooke & Fastook, 2007; Ojala et al., 2019; Peterson-Becher & Johnson, 2021; Vérité et al., 2021), but its extension further up-ice remains unknown. Dow et al. (2014) suggested that subglacial conduits at about 70 km from the Greenland Ice Sheet margin and further upglacier are improbable to maintain because of the high overburden pressure (Figure 16). Murtoos often occur up-flow from eskers formed within the R-channels of the channelised drainage system closer to the ice margin (Ojala et al., 2019) and connect to them via erosional escarpments (Ojala et al., 2022).

Murtoos are primarily depositional landforms with erosional triangular heads (Peterson-Becher & Johnson, 2021). The depositional units of murtoos suggest an increasing influence of subglacial meltwater flow in rapidly widening broad and low conduits with increasing sediment input and transport. We thus suggest that murtoos are indicative of saturated subglacial bed conditions with hyper-concentrated flows or slurries that dominated the last depositional stage of their formation. Eyles (2006) described the transformation of overpressured till into hyper-concentrated slurries as a highly effective erosional tool due to the recharge of meltwater into the ice sheet bed. Brodzikowski & Loon (1991) stated that subglacial conditions, particularly in an environment with an irregular topography, and that water-saturated sediments and instable density gradients, favour the development of mass-transport processes. Closely spaced, narrow and channelised hyper-concentrated flows were probably initiated as subglacial flood pulses under rapidly changing water pressure conditions (Vérité et al., 2021).

Based on the sedimentological evidence presented here, it is proposed that the murtoo body (Unit 2) was deposited during a single melt season because of seasonal variation in meltwater input and to that related changes in the subglacial drainage system. Extra input of meltwater to drive this semi-efficient system must have come from the ice surface or via the drainage of subglacial lakes (Shackleton et al., 2018). The source area of murtoo sediments was undoubtedly upstream of the murtoo head, where the creep of saturated till into a conduit tended to constrict it (Figure 16). Such a zone would include high water pressure and low shear stresses induced from the ice. If till creep was faster than ice flow velocity, subglacial channels cut into the sediment (canals) could exist (Walder & Fowler, 1994). It is usually considered that ice surface slope of the FIS was low (Shackleton et al., 2018). In such a situation, the development of a distributed subglacial canal system would be a stable hydrological configuration with an effective pressure close to zero at the ice/bed interface (Greenwood et al., 2016). The observed weak to moderate, periodic deformation of murtoo sediments induced by overriding ice indicates that the subglacial water pressure (Pw) and the overburden pressure (Pi) were constantly close to each other (Lesemann et al., 2010). This would relate to moderately efficient drainage that could occur through a system close to the overburden pressure (Greenwood et al., 2016).

Murtoo body formation (Unit 2) was most probably initiated by the rapid clogging of the preceding conduits, throttling the flow (Figure 16). In a steady state, the flow of saturated till into the conduit must be balanced by meltwater erosion and transport of the same sediment (Hooke, 2019). Increased water pressures and down-ice-mobilised sediment led to up-ice-migrating lateral erosion of the till and to lateral meltwater flow and erosion around the conduit fill, as reflected by the typical morphology of murtoos (Ojala et al., 2021) (Figure 16). During the murtoo formation, the vertical closure rate was probably highest in the middle and decreased towards the margins (Ng, 1999). Accordingly, melt rates were higher at conduit margins, with the deepest water and greater energy dissipation (Shreve, 1985). In conditions where Pw increased as meltwater discharge (Q) increases, the drainage system would tend to remain braided or distributed (Hooke, 2019). The continuum from murtoo mantle deposition to lateral channel erosion and the final draping of murtoos by boulder blanket suggests development towards route-wide discharge and increased basal melting rates. This could also explain the good preservation of murtoo morphology and suggests a time-transgressive origin for the murtoo fields.

6.2 | A comparison between the sedimentary characteristics of Swedish and Finnish murtoos

Our study presents the typical sedimentary characteristics of triangular-shaped murtoos in the Finnish area of the FIS, which can be compared with those recently excavated and described from Sweden (Peterson-Becher & Johnson, 2021).

Despite some spatial and temporal differences, there are many similarities in sedimentological composition and internal architecture. The most important similarities for both areas include the following: 1) investigated murtoos are characteristically composed of sandy and gravelly diamictons, interbedded with sorted sediments beds (silt, sand and gravel), interpreted as deposited in subglacial position; 2) the murtoo diamictons are relatively loose and semi-sorted in character and with low amounts of finer grain sizes (silt/clay). This deviates from typical subglacial tills, such as traction and basal melt-out tills; 3) in most cases, the sediment in murtoos is found on top of more compact and finer-grained subglacial till; 4) the dominant ductile deformation is restricted to separate beds indicating the periodic nature of deformation events; 5) the contacts between diamictons and sorted beds are mainly gradational and sediments are mostly mixed; 6) there is a frequent, patchy occurrence of sand intra-clasts, which often carry outsized gravel clasts and small boulders; 7) there is a higher abundance of sorted sediments in the lower part of each murtoo, and coarser sediments (including diamicton beds) in the upper part; and 8) in all cases, murtoo surfaces carry a high frequency of large boulders.

A difference, however, is that the Finnish murtoos lack the folding, large-scale convolution and clastic dykes, as described in some of the Swedish murtoos. Swedish murtoos also appear to have been more influenced by liquefaction and exhibit water-escape structures. In general, Finnish murtoos appear to be less deformed, and reveal a tri-partite architecture often with trough-shaped (channelised) diamictons in their upper parts. Finnish murtoos also show current ripples, so far not recorded from Sweden.

It appears that Finnish murtoos were deposited in subglacial environment with an effective pressure close to zero, in which the meltwater input occurred as repeated, short-lived pulses on top of generally high meltwater input. Thus, because of high meltwater pressure, deformation from ice remained low. In spite of this, the sedimentary records from the Swedish examples points to an overall similar sediment composition and internal architecture with the exception of a larger degree of deformation structures, suggesting that the depositional processes of murtoos were highly similar.

7 | CONCLUSIONS

We conclude here that murtoos are depositional landforms with erosional triangular heads. Typically, a murtoo consist of a core with sorted and stratified sediment, followed by deposition of coarser sorted sediment and diamictons, related to mobilisation of saturated sediment during increased meltwater input. Murtoos are thus characteristically composed of clay/silt-poor and semi-sorted heterogeneous diamictons interbedded with coarse gravels, all produced by highly sediment-concentrated flows with intervening low-velocity stream flows and with periodic deformation by the overriding ice. The weak to moderate periodic deformation by the ice indicates a basal effective pressure close to zero due to a high porewater pressure.

The murtoo bodies are proposed to indicate the deposition of the described sediment successions during just one melt season within rapidly widening broad and low conduits or cavities. Murtoo body sediments and the underlying subglacial murtoo core infills together represent a semi-efficient drainage system not recognised before. We suggest that this happened within a zone of high porewater pressure, tentatively about 40–60 km from the ice margin. Our results also suggest that, during the final deglaciation and after murtoo body formation, the subglacial drainage reached route-wide discharge. During this stage was murtoo mantle deposition as well as the final shaping of the murtoos with lateral channel erosion. The boulder-rich murtoo surfaces represent increased basal melting closer to the ice margin. This succession of events, suggesting a time-transgressive development of murtoo tracts, might also explain their good preservation. Importantly, we propose that murtoo tracts within meltwater corridors are a missing element between distributed and channelised drainage systems, not recognised in current glaciohydrological models or even in the theoretical basis of glacial hydrology. The rapid mobilisation of saturated sediment is probably a critical factor in the development of the suggested semi-efficient drainage system. Therefore, understanding of murtoo processes and genesis will have a crucial impact on modelling approaches, as well as on resolving uncertainties associated with the presence of wet subglacial sediment at the ice–terrain boundary and the related development of the drainage system. More research is clearly needed to fully explain the factors influencing the distribution and genesis of murtoos along meltwater routes, as well as their relationship with glacial dynamic conditions and the related development of drainage systems. Furthermore, our results indicate that our understanding of the geomorphological record caused by rapid melting during the last deglaciation of the FIS still merits further investigations.

AUTHOR CONTRIBUTIONS

Mäkinen, J. (a,b,c,d,g,h), Kajuutti, K. (a,b,d,i), Ojala, A.E.K. (a,b,c,d,i), Ahokangas, E. (a,d,i), Tuunainen, A. (d,i), Valkama, M. (d,i), Palmu, J.-P. (d,i).

ACKNOWLEDGEMENTS

This work formed part of the RewarD project (MUST consortium) funded by the Academy of Finland (grant numbers 322243/Joni Mäkinen, University of Turku and 322252/Antti Ojala, Geological Survey of Finland). Special thanks to Niko Putkinen (Geological Survey of Finland) for fieldwork assistance and discussions, and to Juha Davidila and Juha Majaniemi (Geological Survey of Finland) for the GPR surveys and data processing. Thanks to our Swedish colleagues Mark Johnson (University of Gothenburg), Gustaf Peterson-Becher (SGU) and Christian Öhrling (SGU) for fruitful discussions on murtoo genesis. We also want to thank student Katri Ollila for fieldwork assistance in Laihia as well as all the students who participated the fieldwork in Kullaa and Kämmäkkä sites during the geography course LiDAR-based approach on glacial landscapes. Special thanks to the private landowners Hannu Heikkilä, Pentti Härmä, Jarmo Ollila and Ahlstrom company as well as Metsähallitus (state-owned company) for kindly permitting the excavations. Big thanks to anonymous reviewers who

remarkably helped to improve the manuscript. The authors have no conflict of interest.

DATA AVAILABILITY STATEMENT

The data that support the findings of this study are available from the corresponding author upon reasonable request.

ORCID

Joni Mäkinen https://orcid.org/0000-0002-3613-7418

REFERENCES

Ahokangas, E. & Mäkinen, J. (2014) Sedimentology of an ice lobe margin esker with implications for the deglacial dynamics of the Finnish Lake District lobe trunk. *Boreas*, 43(1), 90–106. Available from: https://doi.org/10.1111/bor.12023

Ahokangas, E., Ojala, A.E.K., Tuunainen, A., Valkama, M., Palmu, J.-P., Kajuutti, K., et al. (2021) The distribution of glacial meltwater routes and associated murtoo fields in Finland. *Geomorphology*, 389, 107854. Available from: https://doi.org/10.1016/j.geomorph.2021.107854

Bartholomew, I.D., Nienow, P., Sole, A., Mair, D., Cowton, D., King, M.A., et al. (2011) Seasonal variations in Greenland Ice Sheet motion: inland extent and behaviour at higher elevations. *Earth and Planetary Science Letters*, 307(3-4), 271–278. Available from: https://doi.org/10.1016/j.epsl.2011.04.014896

Brennand, T. (1994) Macroforms, large bedforms and rhythmic sedimentary sequences in subglacial eskers, south-central Ontario: implications for esker genesis and meltwater regime. *Sedimentary Geology*, 91(1-4), 9–55. Available from: https://doi.org/10.1016/0037-0738(94)90122-8

Brodzikowski, K. & Loon, A.J. (1991) *Glacigenic sediments*. Amsterdam: Elsevier.

Chandler, D.M., Wadham, J.L., Lis, G.P., Cowton, T., Sole, A., Bartholomew, I., et al. (2013) Evolution of the subglacial drainage system beneath the Greenland Ice Sheet revealed by tracers. *Nature Geoscience*, 6(3), 195–198. Available from: https://doi.org/10.1038/ngeo1737

Collinson, J.D. & Thompson, D.B. (1993) *Sedimentary structures*, Second edition. London: Chapman & Hall.

Dow, C.F., Kulessa, B., Rutt, I.C., Doyle, S.H. & Hubbard, A. (2014) Upper bounds on subglacial channel development for interior regions of the Greenland ice sheet. *Journal of Glaciology*, 60(224), 1044–1052. Available from: https://doi.org/10.3189/2014JoG14J093

Eyles, N. (2006) The role of meltwater in glacial processes. *Sedimentary Geology*, 190(1-4), 257–268. Available from: https://doi.org/10.1016/j.sedgeo.2006.05.018

Fudge, T.J., Humphrey, N.F., Harper, J.T. & Pfeffer, W.T. (2008) Diurnal fluctuations in borehole water levels: configuration of the drainage system beneath Bench Glacier, Alaska, USA. *Journal of Glaciology*, 54(185), 297–306. Available from: https://doi.org/10.3189/002214308784886072927

Greenwood, S.L., Clason, C.C., Helanow, C. & Margold, M. (2016) Theoretical, contemporary observational and palaeo-perspectives on ice sheet hydrology: processes and products. *Earth-Science Reviews*, 155, 1–27. Available from: https://doi.org/10.1016/j.earscirev.2016.01.010

Hambrey, M.J. (1994) *Glacial environments*. London: University College Press.

Hooke, R.L.B. (2019) *Principles of glacier mechanics*, Third edition. Cambridge: Cambridge University Press.

Hooke, R.L. & Fastook, J. (2007) Thermal conditions at the bed of the Laurentide ice sheet in Maine during deglaciation: implications for esker formation. *Journal of Glaciology*, 53(183), 646–658. Available from: https://doi.org/10.3189/002214307784409243942

Lawson, D.E. (1979) *A sedimentological analysis of the western terminus region of the Matanuska Glacier, Alaska*. Hanover, New Hampshire: U. S. Army Cold Regions Research and Engineering Lab. Rpt. 79–9 122 p.

Lawson, D.E. (1981) Distinguishing characteristics of diamictons at the margin of the Matanuska Glacier, Alaska. *Annals of Glaciology*, 2, 78–84. Available from: https://doi.org/10.3189/172756481794352379

Lehtinen, M., Nurmi, P. & Rämö, T. (2005) *Precambrian geology of Finland*. Amsterdam: Elsevier.

Lesemann, J.-E., Alsop, G.I. & Piotrowski, J.A. (2010) Incremental subglacial meltwater sediment deposition and deformation associated with repeated ice-bed decoupling: a case study from the Island of Funen, Denmark. *Quaternary Science Reviews*, 29(23-24), 3212–3229. Available from: https://doi.org/10.1016/j.quascirev.2010.06.010

Mäkinen, J. (2003) Time-transgressive deposits of repeated depositional sequences within interlobate glaciofluvial (esker) sediments in Köyliö, SW Finland. *Sedimentology*, 50(2), 327–360. Available from: https://doi.org/10.1046/j.1365-3091.2003.00557.x

Mäkinen, J., Kajuutti, K., Palmu, J.-P., Ojala, A. & Ahokangas, E. (2017) Triangular-shaped landforms reveal subglacial drainage routes in SW Finland. *Quaternary Science Reviews*, 164, 37–53. Available from: https://doi.org/10.1016/j.quascirev.2017.03.024

Menzies, J. (1989) Subglacial hydraulic conditions and their possible impact upon subglacial bed formation. *Sedimentary Geology*, 62(2-4), 125–150. Available from: https://doi.org/10.1016/0037-0738(89)90112-7

Ng, F.S.L. (1999) A mathematical model of wide subglacial water drainage channels. In: Wettlaufer, J.S., Dash, J.G. & Untersteiner, N. (Eds.) *Ice physics and the natural environment*, NATO ASI Series I: Global Environmental Change, Vol. 56. Berlin: Springer-Verlag, pp. 325–327 https://doi.org/10.1007/978-3-642-60030-2_26

Nienow, P.W., Sole, A.J., Slater, D.A. & Cowton, T.R. (2017) Recent advances in our understanding of the role of meltwater in the Greenland Ice Sheet system. *Current Climate Change Reports*, 3(4), 330–344. Available from: https://doi.org/10.1007/s40641-017-0083-9

Ojala, A.E.K., Mäkinen, J., Ahokangas, E., Kajuutti, K., Valkama, M., Tuunainen, A., et al. (2021) Diversity of murtoos and murtoo-related subglacial landforms in the Finnish area of the Scandinavian Ice Sheet. *Boreas*, 50(4), 1095–1115. Available from: https://doi.org/10.1111/bor.12526

Ojala, A.E.K., Mäkinen, J., Kajuutti, K., Ahokangas, E. & Palmu, J.-P. (2022) Subglacial evolution from distributed to channelized drainage: evidence from the Lake Murtoo area in SW Finland. *Earth Surface Processes and Landforms*, 2022(12), 1–20. Available from: https://doi.org/10.1002/esp.5430

Ojala, A.E.K., Palmu, J.-P., Åberg, A., Åberg, S. & Virkki, H. (2013) Development of an ancient shoreline database to reconstruct the Litorina Sea maximum extension and the highest shoreline of the Baltic Sea basin in Finland. *Bulletin of the Geological Society of Finland*, 85(2), 127–144. Available from: https://doi.org/10.17741/BGSF/85.2.002

Ojala, A.E.K., Peterson, G., Mäkinen, J., Johnson, M., Kajuutti, K., Palmu, J.-P., et al. (2019) Ice-sheet scale distribution and morphometry of triangular-shaped hummocks (murtoos): a subglacial landform produced during rapid retreat of the Fennoscandian Ice Sheet. *Annals of Glaciology*, 60(80), 115–126. Available from: https://doi.org/10.1017/aog.2019.34

Peterson, G., Johnson, M.D. & Smith, C.A. (2017) Glacial geomorphology of the south Swedish uplands — focus on the spatial distribution of hummock tracts. *Journal of Maps*, 13(2), 534–544. Available from: https://doi.org/10.1080/17445647.2017.1336121

Peterson-Becher, G. & Johnson, M.D. (2021) Sedimentology and internal structure of murtoos — V-shaped landforms indicative of a dynamic subglacial hydrological system. *Geomorphology*, 380, 107644. Available from: https://doi.org/10.1016/j.geomorph.2021.107644

Phillips, E.R. (2006) Micromorphology of a debris flow deposit: evidence of basal shearing, hydrofracturing, liquefaction and rotational deformation during emplacement. *Quaternary Science Reviews*, 25(7), 720–738. Available from: https://doi.org/10.1016/j.quascirev.2005.07.004

Pierson, T.C. (2005) Hyperconcentrated flow – transitional process between water flow and debris flow. In: Jakob, M. & Hungr, O. (Eds.)

Debris-flow hazards and related phenomena. Berlin, Heidelberg: Springer, pp. 159–202 https://doi.org/10.1007/b138657

Piotrowski, J.A., Mickelson, D.M., Tulaczyk, S., Krzyszkowski, D. & Junge, F.W. (2001) Were deforming subglacial beds beneath past ice sheets really widespread? *Quaternary International*, 86(1), 139–150. Available from: https://doi.org/10.1016/S1040-6182(01)00056-8

Pitkäranta, R. (2009) Lithostratigraphy and age estimations of the Pleistocene erosional remnants near the centre of the Scandinavian glaciations in western Finland. *Quaternary Science Reviews*, 28(1-2), 166–180. Available from: https://doi.org/10.1016/j.quascirev.2008.10.003

Powers, M.C. (1953) A new roundness scale for sedimentary particles. *Journal of Sedimentary Research*, 23(2), 117–119. Available from: https://doi.org/10.1306/D4269567-2B26-11D7-8648000102C1865D

Shackleton, C., Patton, H., Hubbard, A., Winsborrow, M., Kingslake, J., Esteves, M., et al. (2018) Subglacial water storage and drainage beneath the Fennoscandian and Barents Sea ice sheets. *Quaternary Science Reviews*, 201, 13–28. Available from: https://doi.org/10.1016/j.quascirev.2018.10.007

Shreve, R.L. (1972) Movement of water in glaciers. *Journal of Glaciology*, 11(62), 205–214. Available from: https://doi.org/10.3189/S002214300002219X

Shreve, R.L. (1985) Esker characteristics in terms of glacier physics, Katahdin esker system, Maine. *Geological Society of America Bulletin*, 96(5), 639. Available from: https://doi.org/10.1130/0016-7606(1985)96<639:ECITOG>2.0.CO;2

Sohn, Y.K., Rhee, C.W. & Kim, B.C. (1999) Debris flow and hyperconcentrated flood-flow deposits in an alluvial fan, northwestern part of the Cretaceous Yongdong Basin, Central Korea. *The Journal of Geology*, 107(1), 11–132. Available from: https://doi.org/10.1086/314334

Sutinen, R., Sutinen, A. & Middleton, M. (2021) Subglacial squeeze-up moraines adjacent to the Vaalajärvi-Ristonmännikkö glacially-induced fault system, Finnish Lapland. *Geomorphology*, 384, 107716. Available from: https://doi.org/10.1016/j.geomorph.2021.107716

Vérité, J., Ravier, É., Bourgeois, O., Bessin, P., Livingstone, S.J., Clarck, C. D., et al. (2021) Formation of murtoos by repeated flooding of ribbed bedforms along subglacial meltwater corridors. *Geomorphology*, 408(3):108248. Available from: https://doi.org/10.1016/j.geomorph.2022.108248

Walder, J.S. & Fowler, A. (1994) Channelized subglacial drainage over a deformable bed. *Journal of Glaciology*, 40(134), 3–15. Available from: https://doi.org/10.3189/S0022143000003750

SUPPORTING INFORMATION

Additional supporting information can be found online in the Supporting Information section at the end of this article.

How to cite this article: Mäkinen, J., Kajuutti, K., Ojala, A.E.K., Ahokangas, E., Tuunainen, A., Valkama, M. et al. (2023) Genesis of subglacial triangular-shaped landforms (murtoos) formed by the Fennoscandian Ice Sheet. *Earth Surface Processes and Landforms*, 1–26. Available from: https://doi.org/10.1002/esp.5606